Corrosion Science 229 (2024) 111854

Contents lists available at ScienceDirect

Corrosion Science

journal homepage: www.elsevier.com/locate/corsci

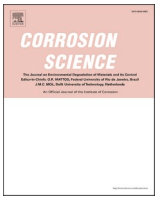

Review

Corrosion inhibition of aluminium alloys by molybdate ions: A critical review of the chemistry, mechanisms and applications

Ingrid Milošev [1,2]

Jožef Stefan Institute, Department of Physical and Organic Chemistry, Jamova cesta 39, SI-1000 Ljubljana, Slovenia

ARTICLE INFO

Keywords:
A. Aluminium
C. Molybdate
C. Corrosion inhibition
C. Passive films
C. Pitting corrosion

ABSTRACT

Molybdate anions are used as an individual inhibitor or in mixed synergistic combinations added directly to the solution, incorporated as fillers, pigments or nanocontainers into various coatings (sol-gel, anodised, plasma electrolytic, organic and layer double hydroxide coatings), as an agent in pre-treatments or post-treatments or as individual conversion coatings prepared to be exposed to aggressive media. The review addresses the action of molybdate on aluminium alloys in each of these applications. The general chemical characteristics of molybdenum are described with a particular emphasis on aqueous chemistry and the formation of monomer and polynuclear species.

1. Introduction

Hexavalent Cr(VI) chromate anions, CrO_4^{2-}, have been traditionally used as corrosion inhibitors and conversion coating formulations for over a century [1–3]. Due to their toxicity and carcinogenicity, their use has been limited and rival options to mitigate corrosion of aluminium alloy are still being explored [4–7]. Molybdate ions have been investigated as a corrosion inhibitor and potential chromate replacement for decades, accumulating quite a comprehensive amount of data. The applications include their use as aqueous corrosion inhibitors, mainly for pitting corrosion but also as additives for cooling systems, inhibitors added to anodisation baths of aluminium, inhibitors against fatigue crack growth, nanoadditives to smart coatings, inhibitors added to the etching solution, or being a part of multilayer combinations. For that reason, a critical literature review on molybdate seems justified since the last review was published quite some time ago by Vukasovich and Farr in 1986 [8], followed by a review on molybdate-based conversion coatings on steel in 2001 [9] and on zinc-based surfaces in 2008 [10]. In this review, the emphasis is given to aluminium and its alloys due to their importance in contemporary technological applications. In the first chapter, the general chemical characteristics of molybdenum and its aqueous chemistry are described. The literature review is organised to show the different actions of molybdate as a corrosion inhibitor in different systems. Molybdate is used as an individual inhibitor or in mixed synergistic combinations added directly to the aqueous or mixed aqueous-alcohol solutions, incorporated as filler, pigments or nanocontainers into various coatings, as an inhibitor added to etching solution and anodisation baths; it is also used in post-treatments or as individual coating prepared to be exposed to aggressive media. The action of molybdate on aluminium alloys in each of these applications is described.

2. General chemical characteristics of molybdenum

Molybdenum is obtained commercially, almost exclusively from roasting molybdenite (MoS_2) [11]. Molybdenum trioxide (MoO_3) is a high-production volume chemical with more than 100,000 tonnes estimated to be produced annually, the majority for direct use in steel production, catalysts and super alloys, solar energy production, etc. Molybdenum is a very base metal, and its domain of stability lies below that of water (Fig. 1) [12]. In the presence of non-complexing acid solutions, Mo dissolves as trivalent ions Mo^{3+}, which is stable only in strongly reducing media. Molybdenum forms two oxides, MoO_2 and MoO_3. In a neutral or slightly acid or alkaline solution, Mo is covered with MoO_2. In tetravalent form, dihydrate and monohydrate were reported, $MoO_2{\cdot}2\,H_2O$ and $MoO_2{\cdot}H_2O$ [12]. By adding concentrated nitric acid to the molybdate solution, yellow hydrated molybdenum(VI) oxide is precipitated, $MoO_3{\cdot}xH_2O$ (also denoted as molybdic acid $H_2MoO_4{\cdot}H_2O$) [12]. It is very slightly soluble in water. In alkaline, MoO_3 is dissolved to form molybdate anions [13]:

E-mail address: ingrid.milosev@ijs.si.
[1] URL https://www.ijs.si/ijsw/K3-en/Milosev
[2] ORCID: https://orcid.org/0000-0002-7633-9954

https://doi.org/10.1016/j.corsci.2024.111854
Received 19 October 2023; Received in revised form 15 January 2024; Accepted 17 January 2024
Available online 20 January 2024
0010-938X/© 2024 The Author(s). Published by Elsevier Ltd. This is an open access article under the CC BY-NC-ND license (http://creativecommons.org/licenses/by-nc-nd/4.0/).

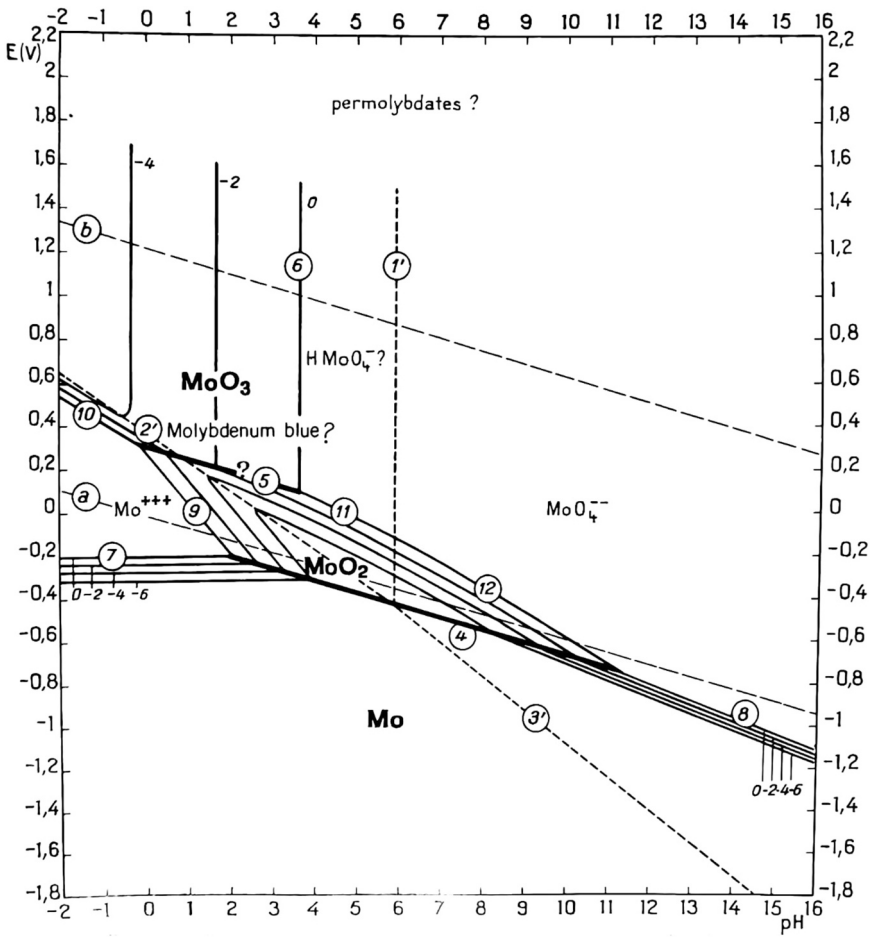

Fig. 1. The E – pH Mo–H_2O diagram at 25 °C [12]. *Reprinted with permission from the book "Atlas of Electrochemical Equilibria in Aqueous Solutions" by Marcel Pourbaix, NACE, Cebelcor (Houston, Brussels), 1974, publisher National Association of Corrosion Engineers* [12].

$$MoO_3(s) + 2OH^- \rightarrow MoO_4^{2-} + H_2O \quad (1)$$

The range of the passivity of Mo is not very broad compared to its neighbours Cr and W from the 6th group, but it extends from low acidic to mild alkaline conditions (pH ~3 –8) (Fig. 1) [12]. The beneficial role of molybdenum in enhancing the stability of chromium oxide-based passive films on stainless steels and Mo-bearing alloys has been known for decades. Maurice and Marcus recently published a comprehensive review of experimental data and density functional theory modelling describing the versatile roles of molybdenum: (i) enriched Mo(VI) species in the outer layer of the passive film act as a barrier impeding the access of Cl^- ions to the inner barrier layer, (ii) Mo(IV) species dispersed at the surface of the inner layer retard the entry of Cl^- ions into the defect sites of the Cr(III) oxide barrier, and (iii) in the Fe-rich compositional defects self-generated by the failure of Cr supply upon initial formation of the barrier layer, molybdenum enhances the selective dissolution of iron and its replacement by Cr(III) and Mo(IV + δ) species [14 and refs therein]. Further, the chemistry of aqueous molybdate anions is complex and offers a broad range of possible chemical and electrochemical reactions, including the formation of monomer and polynuclear species.

2.1. The aqueous chemistry of molybdenum

Molybdenum dissolves in alkaline solutions with the formation of molybdate ions and hydrogen evolution (Fig. 1) [12]. Molybdate (MoO_4^{2-}) anions belong to transition elements under high oxidation states, i.e. V(V), Cr(VI), Mo(VI), W(VI) and Mn(VII) [15]. In their maximum oxidation state, these anions in d^0 electron configuration in an alkaline medium exist as tetraoxo monomers $[MO_4]^{(8-z)-}$. Molybdate anion features a tetrahedral centre; four oxygen are equivalent, with equal bond lengths and angles (Fig. 2**a**) [16]. The length of Mo−O bond is 1.77 Å [17,18].

The speciation of molybdate in aqueous solution is versatile and dependent on pH and molybdate concentration. Fig. 3 presents equilibrium diagrams constructed using the Spana software [19,20] for 0.1 M molybdate in 0.1 M NaCl solution. In aqueous solutions at pH > 6, molybdate exists as tetraoxo MoO_4^{2-} monomers and is a prevailing species.

Upon acidification, at pH < 5, protonated forms of $HMoO_4^-$ and H_2MoO_4 are formed. Polynuclear species can form in acidic pH, especially at higher molybdate concentrations (> 10^{-4} M). Their formation involves a change in coordination from tetrahedral to octahedral. The predominant species is heptamolybdate (paramolybdate), formed according to [15]:

$$7[MoO_4]^{2-} + 8\ H^+ \rightarrow [Mo_7O_{24}]^{6-} + 4\ H_2O \quad (2)$$

Between pH 5 and pH 3, these species coexist with their protonated forms $[HMo_7O_{24}]^{5-}$ (pK = 4.4), $[H_2Mo_7O_{24}]^{4-}$ (pK = 3.5), $[H_3Mo_7O_{24}]^{3-}$ (pK = 2.5). It should be noted that thermodynamic data for Mo species vary depending on the databases used [21].[3]

[3] Thermodynamic data may vary, especially concerning considerable variation in the dominant polynuclear species present at high Mo concentrations and low pH and the range of stability of intermediate $HMoO_4^-$ species. The Organisation for Economic Co-operation and Development (OECD) Nuclear Energy Agency (NEA) Thermochemical Database Project (TDB) is currently running a project of reviewing thermodynamic data on Mo and expected to be published next year.

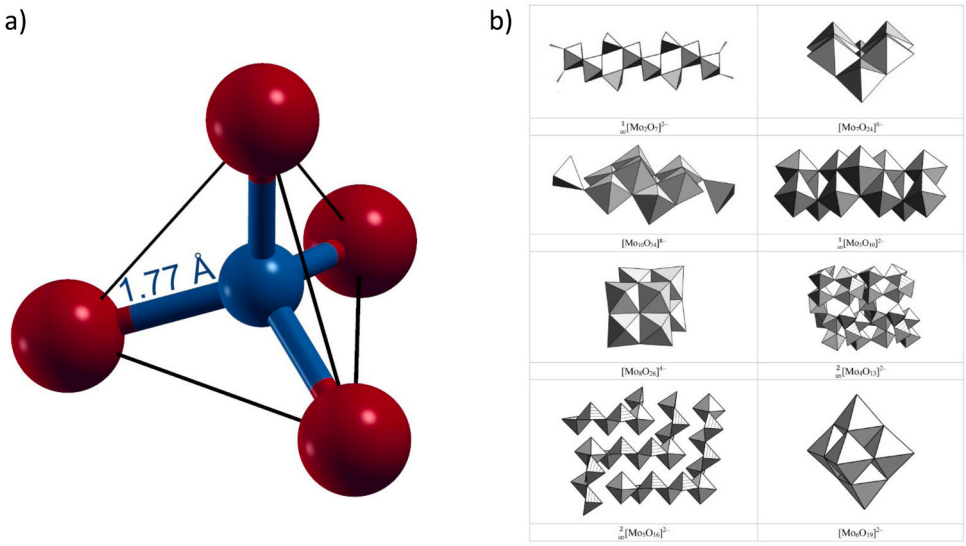

Fig. 2. a) Tetrahedral structure of molybdate ion (courtesy of Prof. Anton Kokalj). b) Polyhedral representations of isopolyoxomolybdate anions. *Reprinted with permission from the publication by H.-J. Lunk and H. Hartl, ChemTexts 7 (2021) 26* [23].

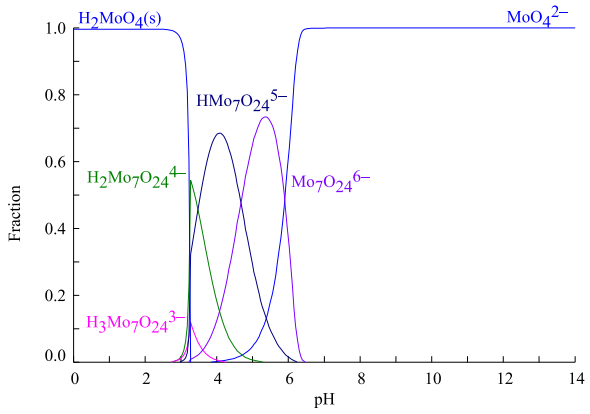

Fig. 3. Fraction diagram of Mo species depending on pH calculated for 0.1 M MoO_4^{2-} and 0.1 M NaCl solution at 25 °C (courtesy of Ana Kraš and Tjaša Pavlovčič).

It is interesting to describe polynuclear species in more detail. Metal ions with oxidation numbers +5 and +6 form in alkaline solution monomeric tetraoxo anions (mono- or orthometalates). When adding a mineral acid to an aqueous solution of their salts, oxo-hydroxo species are formed, followed by polycondensation process. Transition metals oxygen cluster anions thus form polyoxometalates (POMs), which can be divided into isopolyoxymetalates (IPOM) and heteropolyoxometalates (HPOM), depending on whether they contain only transition anion (isopoly-) or additional hetero anion (heteropoly-, e.g. phosphorus or silicon) [15,22,23]. The formation of molybdate IPOMs is written by a net ionic reaction [23]:

$$p[MoO_4]^{2-} + qH^+ \leftrightharpoons \left[H_nMo_pO_{4p-q/2+n/2}\right]^{(2p-q)-} + (q/2-n/2)H_2O \quad (3)$$

where the degree of protonation (Z) is defined by the q/p ratio [23]. IPOM form units built by octahedra, by octahedra and tetrahedra or by octahedra and quadratic pyramids (Table 1). Polyhedral representations of selected IPOMs are presented in Fig. 2**b** [23]. The hexa-, octa- and decamolybdates form discrete oligomeric anions, while the di- and trimolybdates are built up by infinite chains, and the tetra-, penta- and heptamolybdates form infinite layers (Fig. 2**b**) [23].

Under well-defined conditions, IPOMs and HPOMs form giant clusters with more than 300 Mo atoms, which are important functional materials, among them the so-called "Lindqvist structure", "Keggin structure", "molybdenum-blue", "Bielefeld wheel", etc. [22,23].

2.2. Chemical properties and toxicity

The molecular weight of molybdenum trioxide is 143.94 g/mol, and its density is 4.70 g/cm^3 (anhydrous). Its solubility in water is 1.066 g/L (18 °C), 4.90 g/L (28 °C) and 20.55 g/L (70 °C). The molecular weight of molybdenum dioxide is 127.94 g/mol, and its density is 6.47 g/cm^3. It is insoluble.

The molecular weight of sodium molybdate is 205.92 g/mol (anhydrous) and 241.95 g/mol (dihydrate), and its density is 3.78 g/cm^3. Its solubility is 56.2 g/100 mL in cold water and 115.5 g/100 mL in hot water.

Environmental exposures to molybdenum trioxide are negligible [24]. Occupational exposures may occur mainly in mining and metallurgy works, steel foundries, and welding and other hot work processes using steel. The potential human toxicity of molybdate is lower than that of chromate: according to the International Agency for Research on Cancer (IARC), molybdenum trioxide (MoO_3) belongs to the category (Group 2B)[4] in terms of carcinogenicity [24]. In contrast, chromate compound is classified as cancerogenic to humans (Group 1) [25].

According to the Occupational Safety and Health Administration

Table 1
Isopolyoxomolydbate species and their coordination (modified from [23]).

Name	Formula	Coordination
Monomolybdate	$[MoO_4]^{2-}$	Tetrahedral
Dimolybdate	$[Mo_2O_7]^{2-}$	Octahedral / Tetrahedral
Heptamolybdate (para)	$[Mo_7O_{24}]^{6-}$	Octahedral
Decamolybdate	$[Mo_{10}O_{34}]^{8-}$	Octahedral / Tetrahedral
Trimolybdate	$[Mo_3O_{10}]^{2-}$	Octahedral
Octamolybdate	$[Mo_8O_{26}]^{4-}$	Octahedral
Tetramolybdate	$[Mo_4O_{13}]^{2-}$	Octahedral / Quadratic pyramidal
Pentamolybdate	$[Mo_5O_{16}]^{2-}$	Octahedral / Quadratic pyramidal
Hexamolybdate	$[Mo_6O_{19}]^{2-}$	Octahedral

[4] Overall evaluation is that MoO_3 are possibly carcinogenic to humans (Group 2B); there is inadequate evidence in humans for their carcinogenicity but there is sufficient evidence in experimental animals for their carcinogenicity.

Table 2
The comparison of toxicity data between sodium chromate and sodium molybdate.

Compound	LD_{50} oral [mg/kg]	LD_{50} dermal [mg/kg]	LC_{50} inhalation [mg/m^3]	Carcinogenicity
Sodium chromate	136 (rat)	1330 (rabbit)	104 (rat)	Group 2B
Sodium molybdate	4000 (rat)	Not listed	> 2080	Group 1

(OSHA) Hazard Communication Standard (HCS) [26], sodium molybdate (Na_2MoO_4) is not a hazardous chemical [27]. For comparison, sodium dichromate ($Na_2Cr_2O_7$) [28] and sodium chromate (Na_2CrO_4) [29] are classified as hazardous,[5] as categorised by OSHA HCS [26].

It is interesting to compare data on toxicity through lethal dose[6] (LD_{50}) or lethal concentration (LC_{50}) (Table 2). LD_{50} for sodium molybdate is 30 times larger than for sodium chromate [27,29].

3. Molybdate as an aqueous and cooling water corrosion inhibitor

Molybdate has been known as a corrosion inhibitor for over 80 years. The use of molybdate for inhibition purposes was patented in 1939 by Bayes [30], where the corrosion of metals used for cooling systems (iron, copper, brass, solder and aluminium) by the fluid cooling system was shown to be prevented by adding nitrite in combination with tungstic, selenic of molybdic acid. The synergistic effect of molybdate was later confirmed with fluorosilicate to protect aluminium equipment exposed to liquid fertiliser [31]. Vukasovich and Farr reviewed the development of various formulations [8].

Fig. 4 presents the progress timeline in the research field on molybdate as an inhibitor of corrosion of aluminium and aluminium alloys in various applications. The first scientific paper or patent published in the related research field is a milestone from which the research progressed.

3.1. Molybdate as aqueous corrosion inhibitor

The first study published in 1953 dealing with molybdate as an aqueous corrosion inhibitor has been followed by numerous papers, as summarised in Table 3. The inhibition action of molybdate as an aqueous corrosion inhibitor depends on i) molybdate concentration, ii) the ratio between molybdate and chloride, iii) the presence of oxygen, iv) solution pH and v) the type of aluminium alloy. The observed effects are described as follows:

i) The concentraction of molybdate influences the degree of corrosion inhibition. Moshier and Davis reported that the film formed in molybdate solution on aluminium contains several oxidation states; at a fixed pH of 7, the film formed at low molybdate concentrations (10 ppm) is thick and consists of high concentrations of MoO_2, whereas at higher molybdate concentration of 1000 ppm, a thin layer is formed mainly composed of molybdate [32]. The fraction of MoO_3 appeared to be independent of the concentration of molybdate. It was proposed that molybdate selectively impedes the ingress of chloride and limits the growth of the film by restricting the movement of oxygen and hydroxyl ions. At nearly neutral pH, the general observation is that the breakdown (pitting) potential (E_{pit}) is shifted more positive with increasing molybdate concentration; the shift on Al was around 400 mV for the increase in concentration from 0.001 M to 0.1 M Na_2MoO_4 in 0.1 M NaCl [33]. The linear relationship was noted between E_{pit} and the concentration of molybdate [33]:

$$E_{pit} = -0.26 + 0.135 \log c(MoO_4^{2-}) \quad (4)$$

A similar effect was observed in 0.5 M NaCl for the concentration range between 0.0001 M and 0.1 M Na_2MoO_4 [34]. A substantial shift of pitting potential of almost 600 mV in the positive direction was noticed, much broader compared to those observed by the addition of chromate (ca. 290 mV) and tungstate (ca. 200 mV) in the same concentration range [34]. The inhibiting effect of molybdate was ascribed to the adsorption at the Al surface, forming a barrier layer that impedes the ingress of chlorides but also enhances the oxidation of Al, resulting in the stable Al oxide [34]. The most significant shift in E_{pit} was evident with the 0.1 M Na_2MoO_4; concentrations lower than 2.5 mM did not affect the breakdown potential of Al in 0.5 M NaCl [35].

In another study on AA6082, only concentrations above 0.1 M Na_2MoO_4, when added to 0.01 M NaCl, depressed the corrosion current density [36], whereas, on AA2024-T3, the most prominent effect was observed at 125 ppm Na_2MoO_4 (Fig. 5) [37]. As the breakdown potential shifted positively, open circuit potential shifted in the opposite direction, suggesting that molybdate provides the mixed inhibition effect on Al alloys [37]. Notably, the increase in molybdate concentration raises the pH of the solution. In Table 3, pH values are indicated when available.

Two inhibition mechanisms were proposed to protect Al in simulated concrete pore solution, i.e. saturated $Ca(OH)_2$ [38]. When a moderate concentration of 10 mM of molybdate was present, a uniform and compact layer of Al-Ca-Mo(V)-O(H) complexes formed and effectively protected the alloy surface. At a higher concentration of 30 mM, an oxide layer consisting of Al-Mg-Si-O(H) and Al-Ca-Mo(VI)-O(H) formed, where Mg originates from the selective dissolution of the intermetallic particles. At a low concentration of 6 mM, molybdate could not inhibit the corrosion of AA6061 [38].

ii) The extent of inhibition is dependent on the ratio between molybdate and chloride [33,39]. Fig. 6 shows the pitting potential as a function of molybdate concentration in a solution of different chloride concentrations. The lower the chloride concentration, the more positive shift of pitting potential is achieved at the same molybdate concentration. The determination of critical molybdate concentration (c_{crit}) was based on the criterion $E_{pit,\ AA2024\text{-}T3} > E_{OCP,Cu}$, since Cu-containing intermetallic particles (IMPs) are foreseen as the main culprit for localised corrosion. A linear relationship between log c_{crit} and $\log_{Cl}-$ was observed:

$$\log c_{crit} = 0.7 + 1.0 \log c_{Cl-} \quad (5)$$

It was proposed that molybdate retards the chloride ions from reaching the critical concentration for pitting initiation rather than ceasing the chloride ingress [33]. Scully et al. reported an extensive study on the effect of Ce(III), Co(II), Co(III) and Mo(VI) on the localised corrosion of aluminium alloy AA2024-T3 in NaCl solution [39–41]. One of the main findings was that Ce(III) had the lowest critical concentration (defined as the concentration above which inhibition occurs) for Cu plating over Cu-containing IMPs, whereas Mo(VI) has the highest critical concentration but acts as a very potent anodic inhibitor [39–41].

iii) Molybdate is classified as an anodic inhibitor, but it requires the presence of oxygen or other oxidising agent in the solution [42].

[5] Data for $Na_2Cr_2O_7$: Oxidising solid: 2; Acute oral toxicity: 3; Acute dermal toxicity: 4; Acute Inhalation toxicity: 2; Skin Irritation: 1B; Eye irritation: 1; Respiratory senzitation: 1; Skin senzitation: 1; Carcinogenicity: 1B; Germ cell mutagenicity: 1B; Reproductive toxicity: 1B; Specific target organ toxicity (single exposure): 3; Specific target organ toxicity (repeated exposure), where the number represents the category, 1 is the most and 4 the least hazardous. Data for Na_2CrO_4: Acute oral toxicity: 3; Acute dermal toxicity: 4; Acute Inhalation toxicity: 2; Skin Irritation: 1B; Eye irritation: 1; Respiratory senzitation: 1; Skin senzitation: 1; Carcinogenicity: 1 A; Germ cell mutagenicity: 1B; Reproductive toxicity: 1B; Specific target organ toxicity (single exposure): 3; Specific target organ toxicity (repeated exposure), where the number represents the category, 1 is the most and 4 the least hazardous.

[6] Lethal dose (LD_{50}) is the amount of a chemical that is lethal to one-half (50%) of the experimental animals exposed to it.

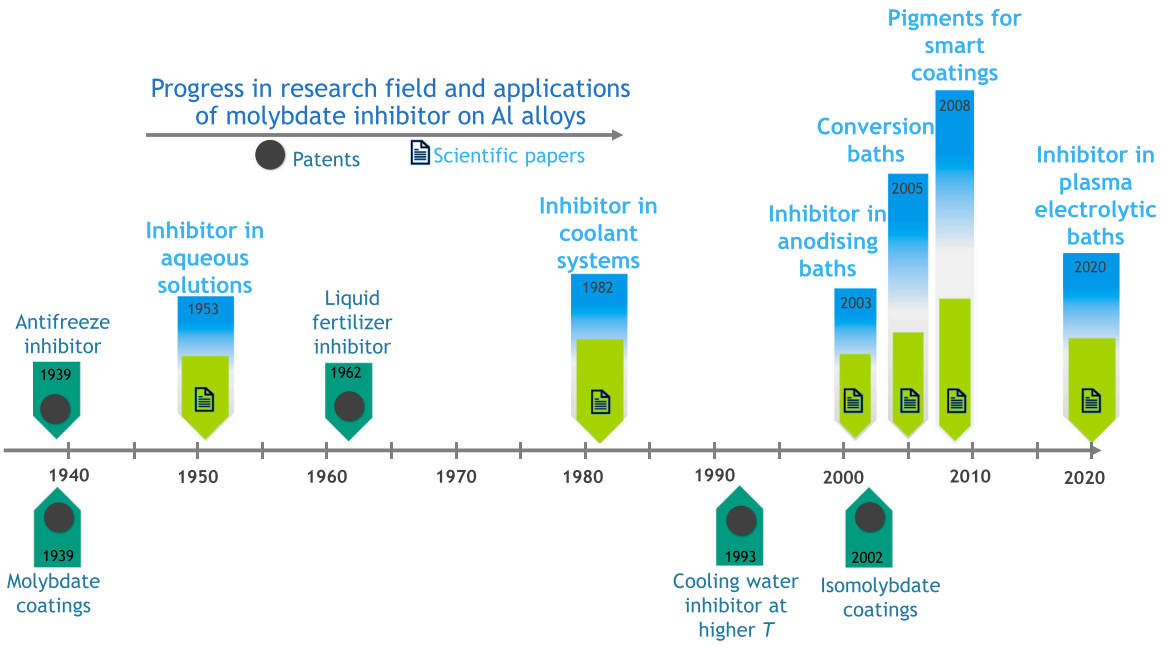

Fig. 4. Progress in the research field on molybdate as an inhibitor of corrosion of aluminium and aluminium alloys presented in a timeline. The first scientific paper or patent published in the related research field is a milestone.

Namely, in contrast to chromate, Mo(VI) is a weak oxidant that requires oxygen, acting as a primary passivator [43]. Pryor and Cohen postulated that relatively strong oxidising anions like chromate and nitrite passivate iron in aerated and deaerate conditions [44]. Weaker oxidising agents such as tungstate and molybdate behave similarly only in the presence of air; in deaerated solutions, these ions do not assure passivity. Oxygen is necessary because molybdate is not a good cathodic depolariser on a clean iron surface but may be more effective on smaller areas when oxygen is present. Molybdate and tungstate could be thus used in systems containing galvanic couples or oxidisable organics where their oxidising character excludes chromate and nitrite [45]. Lopez-Garrity and Frankel reported that the corrosion inhibition of AA2024-T3 by molybdate was effective only in the presence of oxygen [37], in line with earlier studies on steel [42,43].

iv) The effect of solution pH on the inhibitive action of molybdate is associated with the prevailing Mo species at testing pH (Fig. 3). Moshier and Davies pointed out that the chemistry of the passive film is strongly dependent on both pH and concentration [32]. At pH 7, the major constituent of the film is MoO_4^{2-}, which retards the pitting process. However, as the pH increased to 10, MoO_2 formed by the deposition from the solution became the major constituent of the film. It is, however, not capable of retarding the pitting process, which indicates that only molybdate incorporated in the film can act inhibitory and restrict the movements of anions within the film [32].

At pH of solution lower than 7, the inhibitive action of molybdate on Al in chloride solution was suppressed, which was ascribed to the formation of larger polymeric molybdate species not suitable to be accommodated at the flawed regions on the passive layer to induce passivity [33,35]. Further, these polymeric species probably cannot compete with chloride ions during adsorption at the surface, as competitive adsorption between passivating and aggressive species was pointed out as a possible operating mechanism [35]. Among pH values of 3, 7 and 10, the highest film resistance was obtained at near-neutral pH, where both MoO_2 and MoO_3 were formed. At pH 10, an alkaline attack of Al substrate prevails over the inhibition process by molybdate [33].

Badawy and Al-Kharafi studied the effect of molybdate on the passivation of Al, AA6061 and Al-Cu in acidic, near-neutral and alkaline solutions [46–48]. In acidic solution at pH 2, molybdate could passivate the surface, although at a lower extent than chromate [46]. This action was ascribed to the formation of large Mo-polymeric species that could not be incorporated in the flawed regions of the film. In near-neutral solutions, however, the number of flawed regions was reduced in the presence of molybdate, confirming its inhibitive action at this pH [47]. In basic solutions at pH 10, the inhibitive action of molybdate was still operative and ascribed to its reduction to Mo(0) and Mo(III) oxide and their incorporation in the passive film [48].

v) Different inhibitive actions of molybdate on different aluminium alloys are related to the presence of various IMPs. In NaCl containing molybdate, oxygen reduction reaction (ORR) was highly suppressed due to insulating films forming over Cu-rich sites on AA2024-T3 [37,39–41]. Alloying Al with the transition metals and lanthanides (i.e., Al-Co-Ce (-Mo)) is thus the opportunity to improve the resistance of Al alloys to localised corrosion [39]. Natishan et al. showed that alloying Al with Mo shifted the pitting potential of Al more positively. The effect was related to the effect of alloying on the pH of zero charges of an oxide, pH_{pzc}, with the surface having a net negative charge, and cations can be adsorbed at a pH higher than the pH_{pzc} [49].

The power spectral density of electrochemical noise analysis of AA6351 in 0.5 M NaCl was recorded in the absence and presence of sodium molybdate [50]. Molybdate acted as an anodic inhibitor, suppressing pitting corrosion by reinforcing the surface passivating film by incorporating molybdate [50]. Kharitonov et al. investigated the behaviour of AA6063-T5 in molybdate-containing NaCl [51]. Similar to the previous study on AA2024-T3 [37], the inhibition preferentially occurred on IMPs, in the case of AA6063-T5, Fe-rich IMPs, resulting in the formation of mixed Mo(VI, V, IV) species (Fig. 7) [51].

The inhibition effect depends on the inhibitor and type of the alloy. The effect of chromate, molybdate and tungstate on pit formation in chloride solution differed depending on the type of alloy: chromate was a strong inhibitor of pitting corrosion on both AA2024-T351 and AA7050-T7451, but molybdate reduced the degree of corrosion only on the latter [52]. Comparative study of oxo-anions (HPO_4^{2-} and MoO_4^{2-}) and cations (Ce^{+3}, Ce^{+4}, Li^{+}, Mg^{2+}) reported that all these ions were effective as corrosion inhibitors for AA3003, but only Ce ions acted as inhibitors for AA6063 [53].

Summarising, molybdate shows a lower inhibition action at concentrations lower than the threshold concentration of 100 ppm, pH

Table 3
Literature data on using molybdate as a corrosion inhibitor for Al and Al alloys.

Substrate	Solution	Molybdate inhibitor	Reference
Al metal			
Al	hot boiling water, pH 9	4.5 g/L Na_2MoO_4	McCune 1982
Al	Na_2SO_4 w/wo Cl^-, pH 7 – 10	0.1 ppm – 0.1 M Na_2MoO_4	Moshier 1990
Al	1000 ppm NaCl	0.1 M Na_2MoO_4	Shaw 1990
Al	0.5 M NaCl, pH 2, 5, 7	0.0025 M – 0.1 M Na_2MoO_4	Breslin 1994
Al	borate buffer chloride buffer, pH 2	0.01 M Na_2MoO_4	Badawy 1997
Al	borate buffer, pH 4 – 12	0.01 M Na_2MoO_4	Al-Kharafi 1998
Al	borate buffer chloride buffer, pH 7	0.01 M Na_2MoO_4	Badawy 1997
Al	0.5 M NaCl	0.0001 M – 0.1 M Na_2MoO_4	Zein El Abedin 2001
Al	0.1 M Na_2SO_4, 0.1 M NaCl, pH 3, 7, 10	0.001 M – 0.1 M Na_2MoO_4	Emergull 2003
Al	0.05 M – 1 M NaCl, pH 6.5	0.1 mM – 0.1 M Na_2MoO_4	Madden 2013
Al alloys			
A6351	borate buffer, pH 8, + 0.5 M NaCl	0.05 M Na_2MoO_4	Monticelli 1992
AA6061 Al-Cu	borate buffer, chloride buffer, pH 2	0.01 M Na_2MoO_4	Badawy 1997
AA6061 Al-Cu	borate buffer, pH 4 – 12	0.01 M Na_2MoO_4	Al-Kharafi 1998
AA6061 Al-Cu	borate buffer chloride buffer, pH 7	0.01 M Na_2MoO_4	Badawy 1997
AA3003 AA6063	0.1 M $NaHCO_3$ + 0.1 M NaCl	0.05 M Na_2MoO_4	Salghi 2004
AA2024-T351 AA7050-T7451	3.5% NaCl, pH 8.2	0.05 M Na_2MoO_4	Silva 2005
AA2024-T3	borate buffer, pH 7 – 11	0.1 M Na_2MoO_4	Presuel-Moreno 2005
AA2024-T3	borate buffer, pH 7 – 11, 0.005 M NaCl	0.005 M – 0.1 M Na_2MoO_4	Jakab 2005
AA2024-T3	borate buffer, pH 8.2	0.1 M Na_2MoO_4	Jakab 2006
AA2024	0.6 M NaCl, pH 7	3.4 mM Na_2MoO_4	Chambers 2005, 2007, 2008
AA2024	0.6 M NaCl, pH 2, 4, 7, 10, 12	3.4 mM Na_2MoO_4	Chambers 2007
AA6082	0.01 M NaCl, pH 5.5	0.01 M – 0.5 M Na_2MoO_4	Panagopoulos 2009
AA2024-T351 AA7075-T6	0.05 M – 1 M NaCl, pH 6.5	0.1 mM – 0.1 M Na_2MoO_4	Madden 2013
AA2024-T3	0.1 M NaCl, pH 7.1 – 8.3	10 ppm – 150 ppm Na_2MoO_4	Lopez-Garrity 2014
AA6063-T5	0.05 M NaCl, pH 7.2	3 mM $(NH_4)_6Mo_7O_{24}$	Kharitonov 2020
AA6061	simulated concrete pore solution (sat. $Ca(OH_2)$)	6 mM – 30 mM Na_2MoO_4	Wang 2021

lower than 7 and higher than 10 and deaerated condition, while at higher concentrations than the threshold, it is a strong anodic inhibitor, shifting the breakdown potential more positively. This feature is in line with the study by Uhlig and King, who noticed that the Flade potential of iron is increasingly noble for nitrite, chromate, ferrate, molybdate and tungstate [54]. Molybdate also acts as an inhibitor for Al alloys, but the action is governed by the presence of IMPs.

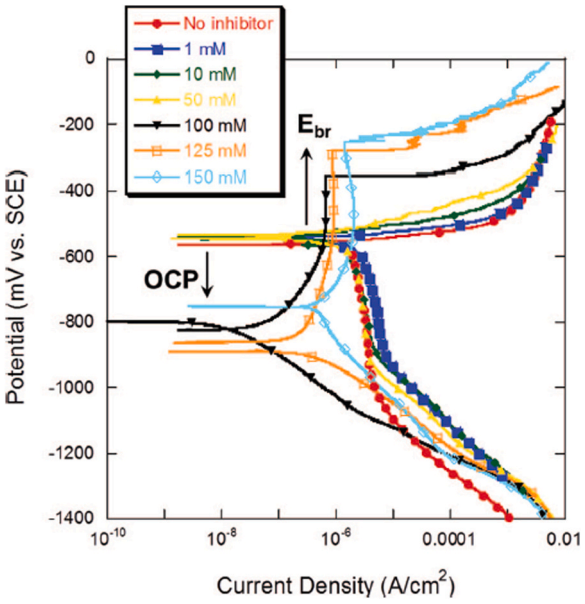

Fig. 5. Polarisation curves for AA2024-T3 in naturally aerated 0.1 M NaCl solution at varying Na_2MoO_4 concentrations. *Reprinted with permission from the publication by O. Lopez-Garrity and G.S. Frankel, J. Electrochem. Soc. 161 (3) (2014) C95 –C106* [37].

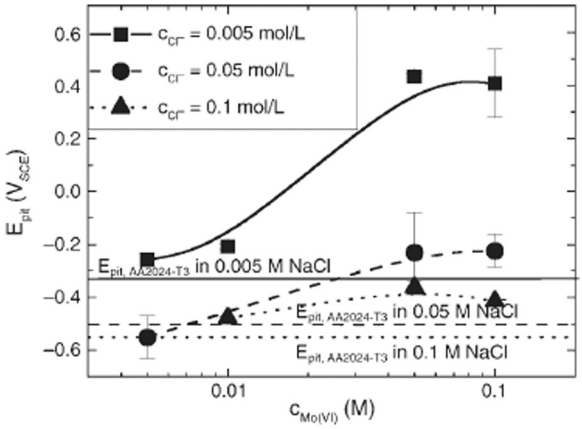

Fig. 6. Pitting potential (E_{pit}) pit as a function of Mo(VI) concentration at different chloride levels. *Reprinted with permission from the publication by M.A. Jakab, F. Presuel-Moreno and J.R. Scully, CORROSION 61 (3) (2005) 246 – 263* [39].

3.1.1. *Proposed inhibition mechanisms*

In the framework of searching for inhibitors suitable for coolant applications, McCune et al. proposed that molybdate and tungstate anions are continuously incorporated into a growing film on Al in hot boiling water, forming a precipitated hydrate aluminium salt of a particular anion rather than pseudo-boehmite which is not self-limiting like in the case of silicate [55]. Baihramov et al., however, concluded that on etched Al surface, Mo exists as both Mo(VI) and Mo(IV) and is not entirely reduced but rather adsorbed, in contrast to dichromate, which is reduced to Cr(III) and incorporated in the film [56].

Based on the literature data, proposed inhibition mechanisms of molybdate are summarised and schematically presented in Fig. 8 separately for Al metal and Al alloys. Let us first consider the inhibition mechanisms proposed on Al metal in near-neutral media containing chlorides. Moshier and Davies postulated that film should contain MoO_4^{2-} to inhibit corrosion [32]. The improvement of pitting resistance was associated with a Mo-rich region of the film surface that inhibited

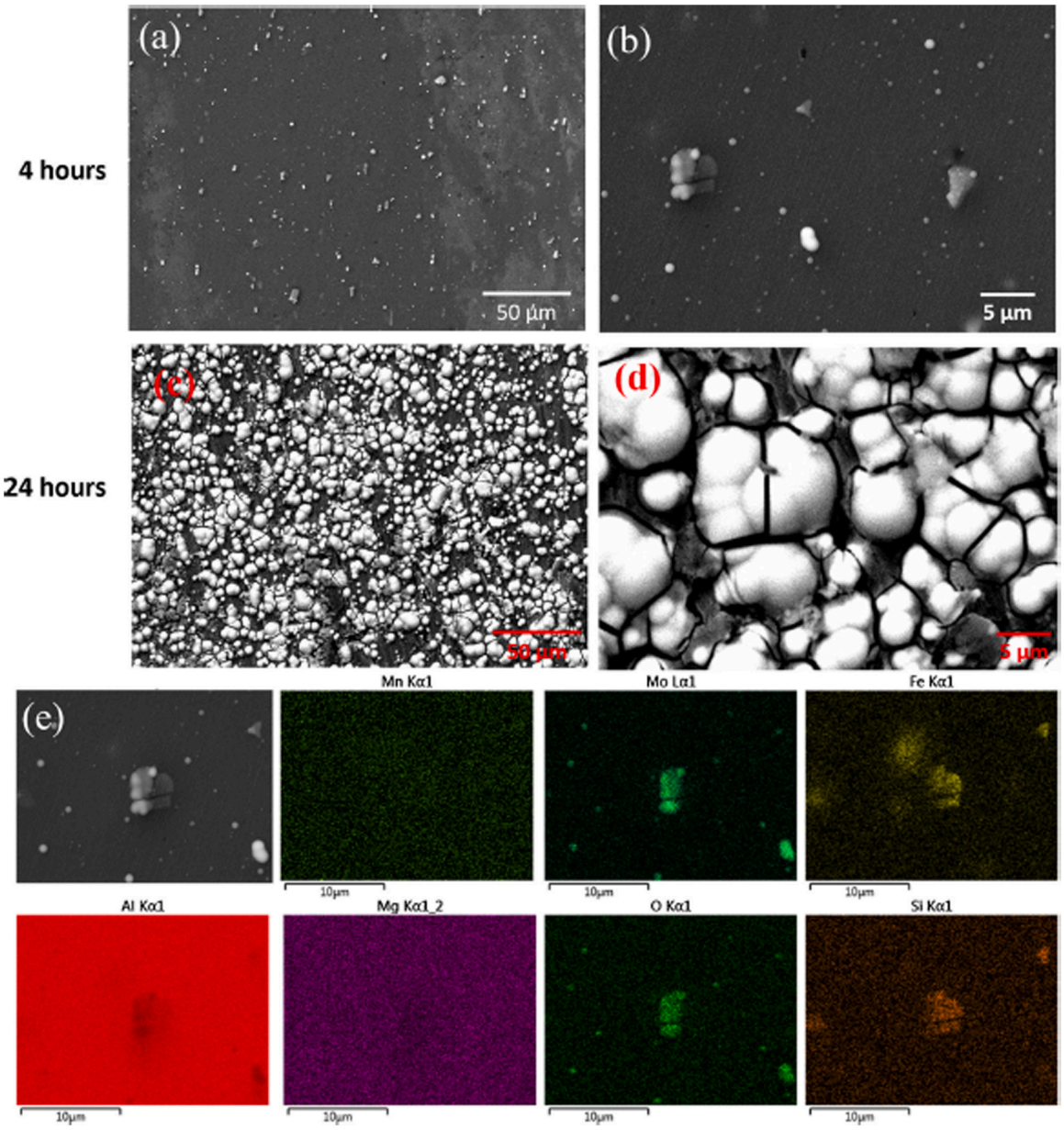

Fig. 7. SEM-EDX surface analysis after 4 and 24 h exposure to 0.05 M NaCl solution with 3 mM $(NH_4)_6Mo_7O_{24}$. *Reprinted with permission from the publication by D.S. Kharitonov, I. Dobryden, B. Sefer, J. Ryl, A. Wrzesińska, I.V. Makarova, I. Bobowska, I.I. Kurilo and P.M. Claesson, Corros. Sci. 171 (7) (2020) 108658* [51].

the ingress of chloride anions. The incorporation of Mo in the layer formed in Na_2SO_4 solution depended on the solution pH and molybdate concentration (as described in the text above) ranging from predominantly MoO_4^{2-} to predominantly MoO_2 as pH increases. The latter compound, however, did not significantly protect the substrate.

Considering that the degree of passivation was dependent on the extent of uptake of the passivating molybdate, as confirmed by several authors in later studies [33,34], Breslin et al. proposed that the inhibition mechanism involves two steps [35]. The first one is the adsorption of molybdate, but only at the flawed region of the oxide film [35]. The adsorbed molybdate then suppresses the adsorption of chloride ions and their ingress through the layer to the substrate. Namely, the initiation of pitting corrosion of aluminium in chloride solutions was postulated to proceed by adsorption of the chloride anions (Fig. 8**a**), chemical reaction with Al^{3+} cations in the oxide lattice and the thinning of the oxide film by dissolution leading to the exposure of metal to the aggressive medium [57]. The chemical reaction leads to the formation of transient complexes [34]:

$$Al^{3+} + 4Cl^- \rightarrow AlCl_4^- \quad (6)$$

$$AlCl_4^- + 2\,H_2O \rightarrow Al(OH)_2Cl + 2\,H^+ + 2Cl^- \quad (7)$$

The incorporation of these complexes leads to the generation of defects or flaws in the Al oxide layer (Fig. 8**a**). These flawed regions of the oxide film are the preferential adsorption sites for anion adsorption (Fig. 8**b**). Following molybdate adsorption, the second step may then occur, that is an oxidation-reduction process, allowing the formation of molybdenum oxide with several oxidation states (Fig. 8**c**) [35]. Although the oxidising ability of molybdate is smaller than that of chromate [34], it still stimulates the oxidation of Al leading to the repassivation of flaws. At the same time, molybdate is reduced. The following reactions were proposed [34,35]:

$$MoO_4^{2-} + 2\,H^+ + 2\,H_2O + 2Al \rightarrow Mo + Al_2O_3{\cdot}3\,H_2O \quad (8)$$

$$MoO_4^{2-} + 5\,H^+ + 2Al \rightarrow Mo^{3+} + 1/2Al_2O_3{\cdot}3\,H_2O + H_2O \quad (9)$$

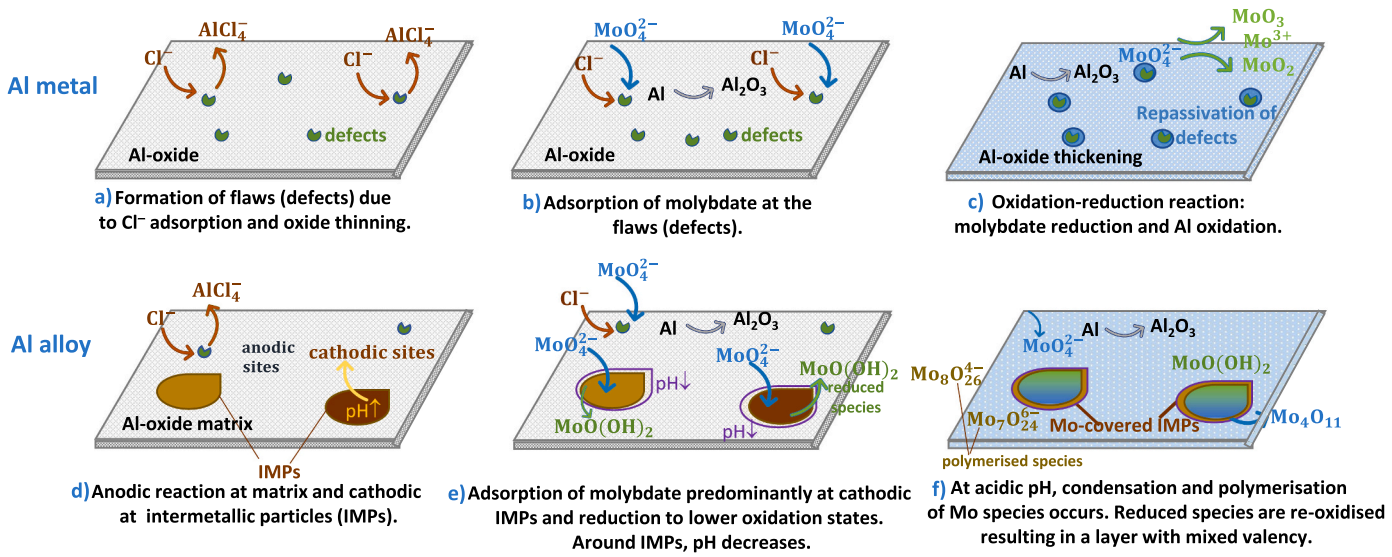

Fig. 8. Schematic presentation of the mechanism of corrosion inhibition by molybdate on Al metal (a-c) and Al alloy (d-f). More details are given in Section 3.1.1.

$$3MoO_4^{2-} + 6\,H^+ + 2Al \rightarrow 3MoO_2 + Al_2O_3{\cdot}3\,H_2O \quad (10)$$

It was also postulated that the molybdate layer formed does not cease the chloride ingress but retards the chloride ions from reaching the critical concentration for pit initiation [33].

Therefore, a simple reduction is insufficient, and molybdate must be incorporated in the layer to achieve passivation. X-ray photoelectron spectroscopy (XPS) analysis showed that the layer formed in the presence of molybdate contained species with different oxidation states, presumably including MoO_2, MoO_4^{2-} and MoO_3 [32,34,46].

In acidic (pH = 2), molybdate inhibited the corrosion of Al but to a smaller extent than chromate [46]. Due to its lower oxidation power and polymeric nature in acidic pH, molybdate forming large species (e.g. $Mo_6O_{21}^-$) cannot form stable passive film free from flawed regions as chromate. The following reaction was reported to occur during immersion [46]:

$$2Al + MoO_4^{2-} + 10\,H^+ \rightarrow Al_2O_3{\cdot}3\,H_2O + 2Mo^{3+} + 2\,H_2 \quad (11)$$

In basic (pH = 10 −12) solutions, chromate was reported superior to molybdate, but the incorporation of molybdate was confirmed by XPS [48]. Aluminium dissolves into soluble complexes (reaction 12), but due to the action of molybdate, the oxidation of Al took place (reaction 13):

$$Al(OH)_{3,ad} + OH^- \rightarrow Al(OH)_{4,sol}^- \quad (12)$$

$$2Al + MoO_4^{2-} + 2\,H_2O \rightarrow Al_2O_3 + Mo_2O_3 + 2OH^- \quad (13)$$

In the second part of this section, aluminium alloys are considered (Fig. 8**d-f**), where the presence of intermetallic particles makes the mechanism of molybdate inhibition even more complex since IMPs represent the sites with different electrochemical activity and oxidation-reduction capacity than the surrounding Al oxide matrix (Fig. 8**d**). At IMPs, cathodic reactions of oxygen reduction and hydrogen evolution take place ($O_2 + 4\,H^+ + 4e^- \rightarrow H_2O$ and $2\,H^+ + 2e^- \rightarrow H_2$), whereas anodic reaction proceeds at the matrix and is related to oxidation of Al to Al^{3+}. Lopez-Garrity and Frankel proposed that the inhibition by molybdate consists of a two-step process (Fig. 8**e**) whereby molybdate is rapidly reduced to $MoO{\cdot}(OH)_2$ over IMPs (reaction 14), which act as local cathodes, thus favouring the reduction of Mo(VI) species [37]. The reduced film was not formed on the matrix, where Al is oxidised to Al (III) oxide (reaction 15). Under the conditions of local acidification, condensation and polymerisation of molybdate species ($Mo_7O_{24}^{6-}$, $Mo_8O_{26}^{4-}$) occur [37]. Reduced species are subsequently oxidised to intermediate oxides (Fig. 8**f**) such as Mo_4O_{11} (reactions 16 and 17) [37].

$$3MoO_4^{2-} + 12\,H^+ + 6e^- \rightarrow 3MoO{\cdot}(OH)_2 + 3\,H_2O \quad (14)$$

$$2Al + 3\,H_2O \rightarrow Al_2O_3 + 6\,H^+ + 6e^- \quad (15)$$

$$8MoO_2 + 6\,H_2O \rightarrow 2Mo_4O_{11} + 12\,H^+ + 12e^- \quad (16)$$

$$5MoO_4^{2-} + 14\,H^+ + 14e^- \rightarrow MoO{\cdot}(OH)_2 + Mo_4O_{11} + 6\,H_2O \quad (17)$$

A similar mechanism was proposed by Kharitonov et al. with the reduction of Mo(VI) to Mo(IV) and subsequent oxidation of reduced Mo (IV) to mixed compound Mo(VI)/Mo(V) [51]. The next step is polymerisation, which can occur only at low pH. The inhibition mechanism over the oxide-covered matrix does not involve the oxidation-reduction mechanism due to its low electrochemical activity, but instead, a thick passivating layer containing polymerised Mo(VI) species is formed [51]. After 4 h of immersion, in 0.05 M NaCl, the surface coverage of the Mo-layer was not homogeneous, but it increased after 24 h (Fig. 7) [51]. The Mo layer was much thicker at IMPs than on the matrix.

The ability of molybdate to suppress the oxygen reduction reaction on copper [40] and AA2024 [41] was confirmed. The MoO_4^{2-} ions can be electrochemically reduced to Mo(IV) on the surface of copper to form chemically insoluble MoO_2, which slows down the ORR kinetics.

Compared to previous studies on Al, these more recent studies on Al alloys involved more powerful surface-analytical techniques for characterising complex Mo-containing layers such as XPS, Raman spectroscopy and scanning Kelvin force microscopy [37,51].

3.1.2. *Inhibition of different types of corrosion attack*

In addition to inhibiting pitting corrosion, molybdate was reported to be effective as a corrosion inhibitor under wear conditions when AA6063 was sliding against stainless steel [36]. Adding molybdate inhibitor led to a decrease in the friction coefficient of the material couple and reduced corrosion current density. Adding molybdate effectively inhibited environmental fatigue crack propagation (EFCP) in peak-aged Al-Cu-Li alloy in chloride solution, establishing itself as a viable chromate replacement inhibitor for this type of corrosion [58]. Hydrogen is a critical parameter in EFCP since it absorbs on the crack tip, diffuses within the fatigue process zone, and causes embrittlement. Molybdate fully inhibited EFCP on Al-Cu-Li alloy, suggesting that a Mo-bearing passive film at the crack tip was a sufficient barrier relative to the required critical hydrogen production and uptake [58]. In another study, molybdate pigments ($CaMoO_4$) added to epoxy coatings were investigated as possible inhibitors for environmental fatigue crack

Table 4
Summary of reported synergistic effects of molybdate.

Substrate	Synergy compound (s)	Conditions	Reference
Al	nitrite	alcohol-water solution + 0.05 to 1 wt% of the alcohol	Bayes 1939
Al	molybdate and nitrate	hot boiling water	McCune 1982
Al	molybdate and phosphate	1 M H_3PO_4 + (1-20 mM) Na_2MoO_4	Li 2011
AA1050	Ce and Al molybdates	0.1 M NaCl + $Ce_2(MoO_4)_3$ + $Al_2(MoO_4)_3$ (0.25 g in 150 mL, pH=6)	Byrne 2023
AA2024-T3	molybdate and silicate	0.1 M NaCl+ (0.1-5 mM) Na_2MoO_4 + (0.1-5 mM) Na_2SiO_3	Lopez-Garrity 2014
AA2024-T3	molybdate and yttrium chloride, cerium chloride, lanthanum chloride and sodium metavanadate	0.6 M NaCl + 3.4 mM total inhibitor	Chambers 2005
AA2024-T3	molybdate and yttrium chloride, cerium chloride, lanthanum chloride and sodium metavanadate	0.6 M NaCl + 3.4 mM total inhibitor	Chambers 2007-2008
AA6061	molybdate and gluconate	3% NaCl + $(NH_4)_6Mo_7O_{24}$ + $C_{12}H_{22}CaO_{14}$	Zhang 2012
AA7075-T76	molybdate and phosphate, citrate, benzimidazole/ benzothiazole derivative (MBTZ)	3.5%NaCl+$Zn_3(PO_4)_3$ + $ZnMoO_4$ (4:1); 3.5%NaCl+$Zn_3(PO_4)_3$ +$ZnMoO_4$ + Ba citrate (8:1:1); 3.5%NaCl+$Zn_3(PO_4)_3$ + $ZnMoO_4$ + Ba citrate + MBTZ (7:1:1:1);	Liu 2002

growth instead of chromate; however, they proved inefficient when used as such [59] opposite to as added to a bulk solution [58].

Madden et al. reported a comparative study on the ability of chromate and molybdate ions to repassivate scratch area on Al, AA2024-T351 and AA7075-T6 [60]. While chromate was found to suppress scratched electrode current transients at high potentials on both alloys, molybdate did not suppress current transients, but the rapid growth of a passive film was observed [60].

3.1.3. The synergy of molybdate with other ions as an aqueous corrosion inhibitor

Another interesting issue concerning molybdate is the possibility of a synergistic combination. The synergism of molybdate with other inhibitor species and in different systems was identified – as aqueous inhibitors or nanocompounds added to coatings. Synergy in nanocompounds is discussed in section 4.2. Here, the synergy of molybdate added as an aqueous inhibitor is considered. The main results are summarised in Table 4.

Synergy occurs when inhibition by the combination of compounds exceeds that of individual compounds. This is especially interesting concerning the REACH directive[7] since synergistically combining already registered compounds is more desirable than registering new ones. The inhibition synergy of various combinations of compounds has been addressed by high-throughput experiments conducted using direct current polarisation applied between two AA2024-T3 electrodes and a multiple-electrode testing system [61–64]. The resulting current was measured over 9 h in 0.6 M NaCl and taken as a screening parameter [61]. The synergy of molybdate with metavanadate and rare earth cations (added as yttrium, lanthanum and cerium salts) was identified, even outperforming chromate anions [61]. In addition to the resulting current, other screening parameters relevant during multiple-electrode testing were selected, i.e. surface Cu enrichment (due to dealloying of Cu-rich intermetallic particles) [62] and dissolved Al ions [63,64]. All these parameters confirmed the synergistic action of molybdate and metavanadates as anodic inhibitors and rare earth cations as cathodic inhibitors.

The molybdate-nitrite combination is also efficient, as shown in antifreeze liquid and other systems [8,30], with nitrite being a known anodic oxidising inhibitor for ferrous and non-ferrous metals. Synergy was noted between molybdate and nitrate; when nitrate was added to molybdate, the extent of growth of oxide film on Al in hot boiling water increased [55].

Strong synergistic behaviour was observed when AA2024-T3 was immersed in 0.1 M NaCl solution containing Na_2SiO_3 and Na_2MoO_4 [65]. When adding molybdate to silicate, the threshold concentration for corrosion inhibition was lower; it was proposed that molybdate preferentially reduces over IMPs during the early stages of corrosion, forming MoO_2. During that stage, the Al matrix dissolves due to pH increase, forming aluminosilicate film, which protects the surface from pitting corrosion breakdown [65]. Molybdate was reported to anodically inhibit the corrosion on Al in 1.0 M H_3PO_4 [66]. Good inhibition efficiency was ascribed to a synergistic action of molybdate and HPO_4^{2-} to produce heteropolyacid ions [66]:

$$12MoO_4^{2-} + HPO_4^{2-} + 23\ H^+ \rightarrow [P(Mo_{12}O_{40})]^{3-} + 12\ H_2O \quad (18)$$

These heteropolyacid ions can adsorb on the positively charged Al surface and form complexes with Al ions, producing a protective film [66]. The synergy of molybdate with, e.g. phosphate and silicate, is based on the possibility of the formation of heteropolymolybdate containing Mo species of different oxidation states and hetero atoms such as phosphorus or silicon [15]. In addition, phosphate ions promote precipitation of insoluble products [67].

Corrosion protection of AA7075-T76 was tested during immersion for 120 h in 3.5% NaCl with different individual inorganic and organic inhibitors and their mixtures [68]. As inorganic inhibitors, zinc phosphate $Zn_3(PO)_4$, zinc borate $3ZnO{\cdot}2B_2O_3$ and zinc molybdate $ZnMoO_4$ were used. As organic inhibitors, barium citrate, barium salicylate—belonging to carboxylates—and benzimidazole/benzothiazole derivative (MBTZ). The best performance was achieved by combining phosphate, molybdate, citrate and MBTZ, which provided inhibition of general and localised corrosion. Citrate and MBTZ formed a chemisorbed layer on oxide films and IMPs. Citrate has three carboxylic groups, which can strongly adsorb to the surface, whereas MBTZ contains sulphur and nitrogen and is known as an inhibitor for Cu, here being one of the main culprits for increased cathodic activities in IMPs on Al alloys. The adsorption of citrate and MBTZ lowered the reactivity of the Al alloy surface and facilitated further passivation by molybdate. At the same time, phosphate, which reacts with corrosion products that deposit on the surface of the metal, forms a protective film and provides long-term inhibition [68].

The synergistic effect was noticed between ammonium molybdate, $(NH_4)_6Mo_7O_{24}$, and calcium gluconate, $C_{12}H_{22}CaO_{14}$, when added to 3% NaCl [69]. Electrochemical measurements on AA6061 alloy suggested that the adsorption of $(NH_4)_6Mo_7O_{24}$ was promoted by adding $C_{12}H_{22}CaO_{14}$ in the solution. In another study, cerium and aluminium molybdate compounds, $[Ce_2(MoO_4)_3]$ (CeMo) and $[Al_2(MoO_4)_3]$

[7] Regulation, Evaluation, Authorisation and Restriction of Chemicals is a EU regulation which addresses the production and use of chemical substances and their impact on humans and environment.

(AlMo), were first synthesised and then tested as corrosion inhibitors added to 0.1 M NaCl [70]. Both compounds achieved strong corrosion protection of AA1050. The idea of binary mixtures is to combine the cathodic inhibitors such as Ce(III) and Al(III) with anodic inhibitor Mo (VI), thus achieving a high mixed corrosion inhibition [70].

3.2. Molybdate as a corrosion inhibitor in cooling water

The original patent from 1939 aimed to use molybdate as a corrosion inhibitor for all metals of a cooling system of the internal combustion engine [30]. A coolant is necessary to transmit the produced heat to an external environment without overheating the engine. As coolants, alcohols are usually added to water to prevent it from freezing during the cold cycle. Among alcohols, ethylene glycol ($C_2H_6O_2$) is most common. The corrosion resistance of Al alloys can be jeopardised in such systems by elevated temperature, chloride ions and other contaminants [71]. Various inhibitors were considered to inhibit corrosion of Al alloys in ethylene-glycol mixtures: sodium nitrite, sodium nitrate, sodium molybdate and sodium silicate were added to the water and ethylene glycol (33%) mixture and reported that sodium nitrate exhibited the best performance on AA3003 with and without galvanic coupling [72]. Similar results on the prevalence of nitrate over molybdate were found in another study tested under static and laminar conditions simulating the hydrodynamic conditions of automotive cooling systems [73]. However, the reason for the superiority of nitrate over molybdate may be that these ions were not tested in a synergistic mixture, as proposed by the original patent [30], and as used in commercial coolants. The feasibility of enhancement of pitting corrosion resistance of AA6351 was investigated by immersion in degraded propylene glycol/water solution at 80 °C for 60 days [74]. Sodium molybdate added at concentration 0.01 M reduced the pitting corrosion initiated by the spots where copper re-deposited after selective dissolution from the alloy. The action of molybdate hindered the cathodic action of copper ions and inhibited the anodic dissolution of aluminium [74].

Notably, the mechanism of molybdate action in ethylene-glycol mixtures is scarcely investigated in academic literature, contrasting its efficiency in versatile commercial cooling systems and technical patent literature such as ref [75]. Further insight into the mechanism is required in future studies.

4. Molybdate as a corrosion inhibitor in coating systems

Molybdate ions have been used individually or in synergistic combinations incorporated as layer double hydroxides pigments or Mo-based nanocontainers into various coatings.

4.1. Mo-containing layer double hydroxides added to coatings

Layered double hydroxides (LDHs) are recognised as lamellar inorganic materials with a brucite-like structure similar to hydrotalcite [76,77]. They comprise consecutive layers of divalent metal hydroxides and trivalent metal hydroxides coordinated with hydroxide groups and held together by van der Waal's forces [77]. Partial substitution of divalent cation fraction by trivalent cations results in a positive sheet charge, compensated by anions in the interlayer galleries. The common formula of LDH is $[M^{2+}_{1-x}M^{3+}_{x}(OH)_2]^{x+}\ [A_{x/n}]^{n-}\cdot yH_2O$, where M^{2+} and M^{3+} are divalent and trivalent metal cations (e. g. Mg^{2+}, Ca^{2+}, Zn^{2+}, Al^{3+}, Cr^{3+}, Fe^{3+}, etc.), respectively, A is an interlayer anion with charge n^- and x is the molar ratio $[M^{3+}/M^{2+}+M^{3+}]$ [77]. Due to their ion-exchange capacity, LDHs offer a great potential to incapsulate inhibitors and release them when necessary – due to the dissolution of LDH framework at extreme pH values or anion exchange within the LDH [78]. The corrosion process can invoke a change in pH, so this principle is used in so-called smart coatings for active corrosion protection.

In one study, LDH layers were intercalated with inhibitors and then used as individual layers deposited on AA2024 substrate [79]. AA2024 samples were immersed vertically in $Zn(NO_3)_2{\cdot}6\ H_2O$ and NH_4NO_3 mixture for 6 h at 45 °C. Subsequently, ZnAl LDH-coated substrates were immersed in 2-mercaptobenzimidazole (MBI), vanadate or molybdate solutions for intercalation. All intercalated inhibitors provided enhanced corrosion protection measured in 0.05 M NaCl and salt spray chamber [79].

In most studies, however, LDH particles were filled with molybdate (or other inhibitors) and then added to a coating to incorporate pigments for increased inhibition action. LDHs filled with inhibitors can be used as pigments loaded in organic and hybrid sol-gel coatings. Montemor et al. explored epoxy primers loaded with hydrocalcite LDHs filled with MBI or cerium molybdate nanospheres filled with MBI [80]. When these doped primers were deposited on galvanised steel, both nanocontainers inhibited artificially induced defects, indicating self-healing ability [80]. Another concept was tested in zinc-aluminium-cerium (ZnAlCe) LDH nanocontainers filled with molybdate or vanadate; these doped nanocontainers were then embedded in hybrid sol-gel coating based on silicon and zirconium and deposited on AA2024 [81]. After immersion in chloride solution, molybdate and vanadate were rapidly released and reached a plateau. Active inhibition and exchange behaviour of LDHs enabled self-healing properties, with vanadate achieving better results than molybdate [81]. A similar concept was used by Subasri et al. but with ZnAl LDHs intercalated with various corrosion inhibitors (phytic acid, molybdate, vanadate, MBI and 8-hydroxyquinoline (8-HQ)) and embedded in Si-Zr sol-gel coating deposited on AA2024-T3 [82]. All doped sol-gel coatings exhibited better corrosion protection than bare coatings and were superior to chromate coatings [82].

The kinetics of the release of molybdate from Mg-Al LDHs containers filled with molybdate was studied using the design-of-experiments method [83]. LDH containers were then added to the polyvinyl alcohol (PVA) matrix and deposited on AA5054. pH as the processing parameter has a significant effect on the molybdate release; it is not clear, however, from the data given, how the release was measured.

Bendinelli et al. used ion chromatography to measure the release of molybdate encapsulated in Mg-Al LDH depending on the reconstruction route used for synthesis [84]. Hydrocalcite was calcinated, reconstructed in different media and then the substitution of interlamellar anions with molybdate was made. The molybdate release was faster when hydrocalcite was reconstructed with glycerol and slower for terephthalate (after 24 h, both released approximately 5000 ppm), indicating that the rate of release may be modulated by the reconstruction route [84].

4.2. CeMo nanowires and nanocontainers added to coatings

Yasakau et al. synthesised CeMo nanowires and embedded them in a Si/Zr hybrid sol-gel coating deposited on AA2024-T3 [85–87]. The suppression of local corrosion activity in artificial defects was observed due to the combined action of Ce and Mo inhibitors (Fig. 9) [86]. When synthesised, CeMo nanowires are amorphous but transform into crystalline phases during immersion in chloride solution, releasing Ce and molybdate species [87]. It was shown that molybdate significantly inhibits the active dissolution of Al and Mg from the S-phase, thus reducing dealloying process. The main role of cerium cations is to mitigate the cathodic process on partially dealloyed intermetallics at the later stages of corrosion [87].

Dias et al. used sol-gel coating modified by La- and Mo-enriched zeolite microparticles [88]. When deposited on AA2024-T3, such coating enabled the "on-demand" release of Mo and La ions from loaded zeolite triggered by the adsorption of Mg^{2+} and Cu^{2+} ions from dissolving IMPs. This step is followed by forming a Mo-Na-La compound on IMPs, which mitigates further dissolution [88].

CeMo nanocontainers were filled with corrosion inhibitors and embedded in epoxy coatings deposited on AA2024-T3 [89,90]. CeMo nanocontainers were filled with MBI [89] or 8-HQ and

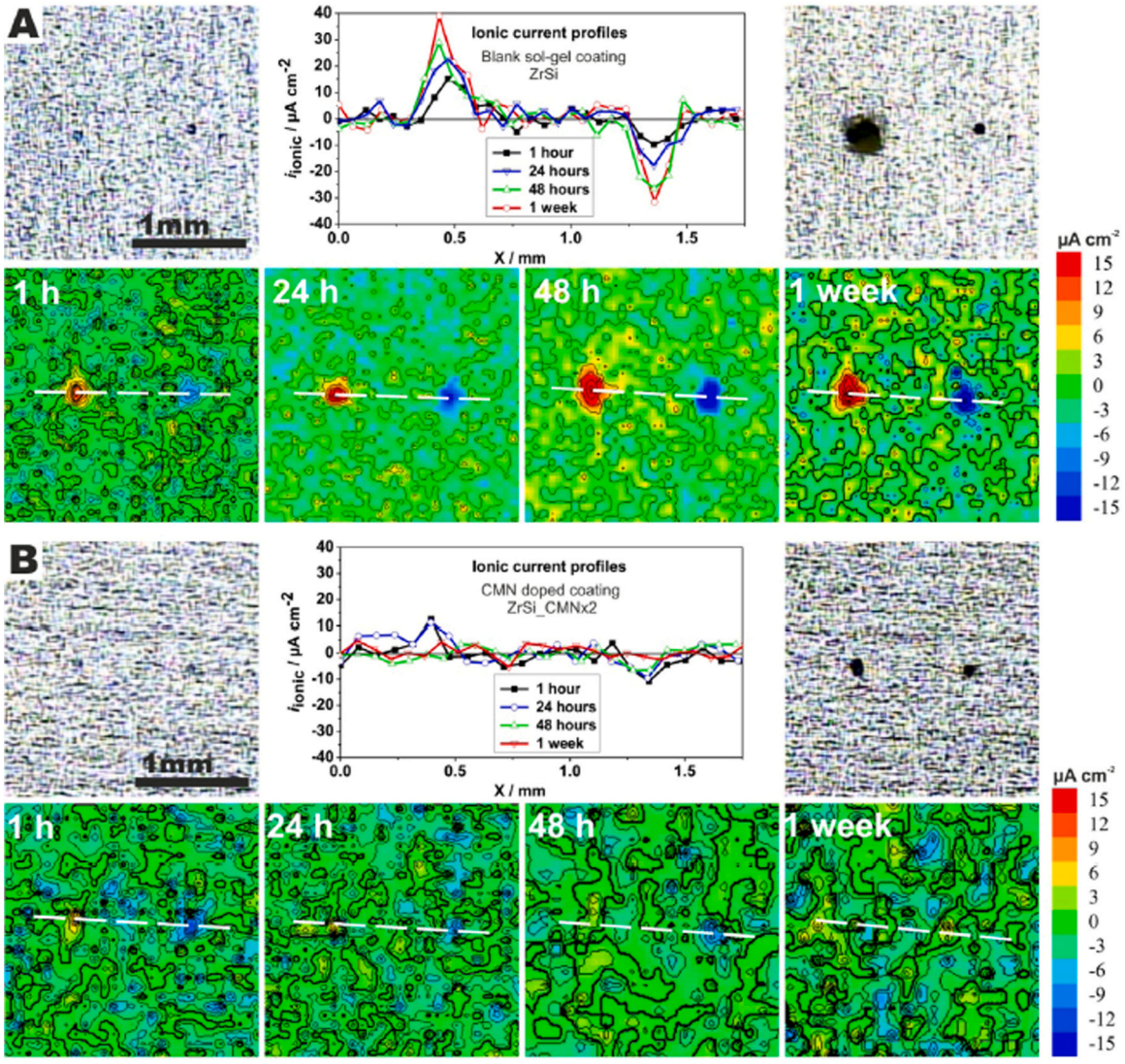

Fig. 9. Optical photographs, scanning vibrating electrode technique (SVET) maps and selected profiles of ionic currents representing the maximal anodic and cathodic activities at artificial defects during 7 days of immersion in 0.5 M NaCl corrosive media. Blank sol-gel coating (a) and sol-gel coating doped with cerium molybdate nanowires (CMN) (b). *Reprinted with permission from the publication by K.A. Yasakau, S. Kallip, M.L. Zheludkevich and M.G.S. Ferreira, Electrochim. Acta 112 (12) (2013) 236 – 246* [86].

1-H-benzotriazole-4-sulphonic acid (1-BSA) [90]. All inhibitors were reported to improve the corrosion resistance and prolong it over almost one month [89,90]. CeMo nanocontainers filled with 2-mercaptobenzothiazole (MBT) were used as nanoadditives together with multi-walled carbon nanotubes and titanium carbide particles in the hybrid sol-gel coatings deposited on friction stir-welded AA6082-T6 and AA5083-H111 alloys [91]. The role of CeMo nanocontainers was to release the MBT inhibitor but the container shell also acted as an inhibitor by adsorption of polymolybdate species onto the surface of Al alloys and forming a protective layer as well as by deposition of cerium oxide films on the cathodic sites [91].

However, incorporating inhibitors into sol-gel coatings is not trivial, as reported for sol-gel coatings incorporated with various inorganic inhibitors, among them molybdate [92]. The morphology and solubility of sol-gel coating play an important role since inhibitor additives can decrease the stability of the sol-gel network and, if too soluble, lead to a rapid loss and release from the coating.

5. Molybdate as a corrosion inhibitor in anodisation baths

Anodic oxidation and plasma electrolytic oxidation are electrochemical surface treatments for modifying aluminium and aluminium alloys to increase their mechanical properties and corrosion resistance [93]. The latter is based on forming a non-conductive oxide layer layer with a high dielectric constant.

5.1. Anodic oxidation

In anodic oxidation, the sample to be oxidised is set in an electrochemical cell and connected to DC power, typically operating between 20 and 80 V and at low current density (1 –10 A dm^{-2}). Acidic electrolytes, either sulphuric or chromic, were commonly used. The trend of replacement of chromic acids due to the carcinogenicity of Cr(VI) has dictated the use of other and more environmentally friendly acids. Two major groups include (i) phosphoric acid-based and alkaline electrolytes and (ii) sulphuric acid-based electrolytes, often mixed with organic acid electrolytes such as tartaric, oxalic, malic, malonic and citric acids [94]. Anodisation produces an oxide layer on aluminium alloys consisting of a thin barrier layer and a thicker porous layer up to 10 μm thick. Due to their porous nature, layers produced by anodic oxidation are sealed – either by immersing in hot deionised water, or sulphate- and acetate-based solutions [93].

Several studies have explored molybdate as a corrosion inhibitor added to the anodising bath. Anodic layers prepared on AA2024 in sulphuric acid containing different molybdate concentrations were tested in NaCl solution [95,96]. When prepared at low molybdate concentration (< 0.1 M), the inhibition effect was not pronounced, but at higher concentrations, the formed layers expressed good corrosion resistance [95,97]. The difference was explained by the effect of acidic pH at lower molybdate concentrations and the formation of polynuclear species, which are not protective. With increasing molybdate concentration, stable molybdate compound was incorporated into the oxide layer, assuring additional protection [95]. When added to the tartaric/sulphuric anodising bath for AA2024-T3, molybdate did not affect the porous anodic film morphology but resulted in the incorporation of molybdate species in the porous skeleton and improved corrosion resistance [98].

Molybdate was considered as a replacement of chromate inhibitor in orthophosphoric acid baths [66]. Its inhibitive action was ascribed to the adsorption and further condensation to polymolybdate species accompanied by the synergistic action of phosphate anions (reaction 18). These heteropolyacid ions then complex with Al^{3+} ions, forming a protective film at the Al surface. Kwolek et al. studied the inhibition mechanism of molybdate in orthophosphoric acid for anodisation of Al [99,100] and Al alloys AA2024 [101] and AA7075 [102]. The mechanism proposed by Li et al. [66] was further modified to involve two stages: adsorption of polycondensed species, presumably $PMo_{12}O_{40}^{3-}$, on the Al surface followed by the formation of a well-adherent Mo-based conversion coating with a typical dry-mud morphology. When using 50 mM MoO_4^{2-} in 1 M H_3PO_4 bath, molybdate can be successfully applied to replace CrO_4^{2-} in the solution. Spectrophotometric studies indicated that at least two species formed during the reduction of molybdophosphoric acid with Al, but their exact composition is challenging to specify and dependent on the initial concentration of molybdate [99].

Molybdate inhibits the corrosion of AA2024 and AA7075 in orthophosphoric acid, but the mechanism is more complex than that of pure Al due to the localised corrosion around intermetallic particles. Nonetheless, heteropolyoxymolybdate species act as anodic corrosion inhibitors, whereas the formation of blue phosphomolybdenum species ($PMo_{12}O_{40}^{7-}$) is undesirable since they do not inhibit corrosion.

An interesting application was reported for the use of molybdate for superhydrophilic modification and enhanced corrosion resistance method of Al alloy 5052 applied in low-temperature multi-effect distillation (LT-MED) seawater desalination system, as the most promising thermal desalination technology for seawater [103]. The surface properties of the desalination tube of the LT-MED system are crucial – they should be superhydrophilic to allow efficient heat and mass transfer, as well as a self-cleaning and bio-foul barrier. At the same time, such a surface has to be corrosion resistant in highly corrosive environments (hot and humid, 60 −70 °C) since most failures occur due to corrosion. Superhydrophilic and corrosion resistance properties were optimised by tuning the anodisation parameters in pyrophosphoric acid by adding Na_2MoO_4 (Fig. 10). The contact angle of water drop below 5° was attained, and excellent corrosion resistance was measured in 3.5 wt % NaCl at 70 °C. The action of the inhibitor was ascribed to the absorption of the porous layer, thickening of the barrier layer, and Mo(VI) incorporation [103].

5.2. *Plasma electrolytic oxidation*

Plasma electrolytic oxidation (PEO) technique (also called micro-arc oxidation, plasma chemical oxidation and anodic oxidation by spark discharge) was developed to overcome some drawbacks of anodisation, primarily to improve the corrosion resistance and mechanical properties. Compared to anodisation, much higher voltages are used (400–700 V) and greater than the dielectric breakdown voltage. The power source can be DC, AC, unipolar pulsed or bipolar pulsed mode. Common electrolytes for the PEO of aluminium in alkaline media (pH 7–12) are silicates, phosphates, aluminates, fluorides, etc.) [104]. The electrode is first anodised to produce a thin barrier layer, followed by the stage where the dielectric breakdown begins, accompanied by ionisation of the oxide materials and gas evolution. The layers have a three-layer structure, with an inner barrier layer, a compact working layer and a loose outer layer (so-called technological layer). Produced layers consist of a complex mixture of amorphous and crystalline phases of aluminium oxides up to 200 μm thick, with a high hardness and superior adhesion to the substrate.

Usually, many pores and cracks are formed within the coating; furthermore, the process is energy-consuming, with a typical treatment lasting up to 1 h. Recently, flash-PEO coatings were developed where only thin coatings are produced (1 −5 μm) due to several minutes of treatment. One of the possibilities to increase the corrosion resistance of flash-PEO coatings once exposed to an aggressive medium is to incorporate corrosion inhibitors [105]. The possibility of ionic migration under the electric field and plasma-chemical reactions in the micro-discharge channels should facilitate this. Del Olmo et al. loaded flash-PEO coatings with different anodic and cathodic inhibitors in the presence of EDTA [105]. Among anodic inhibitors, tungstate was superior to molybdate and vanadate. Cathodic inhibitors like rare earth

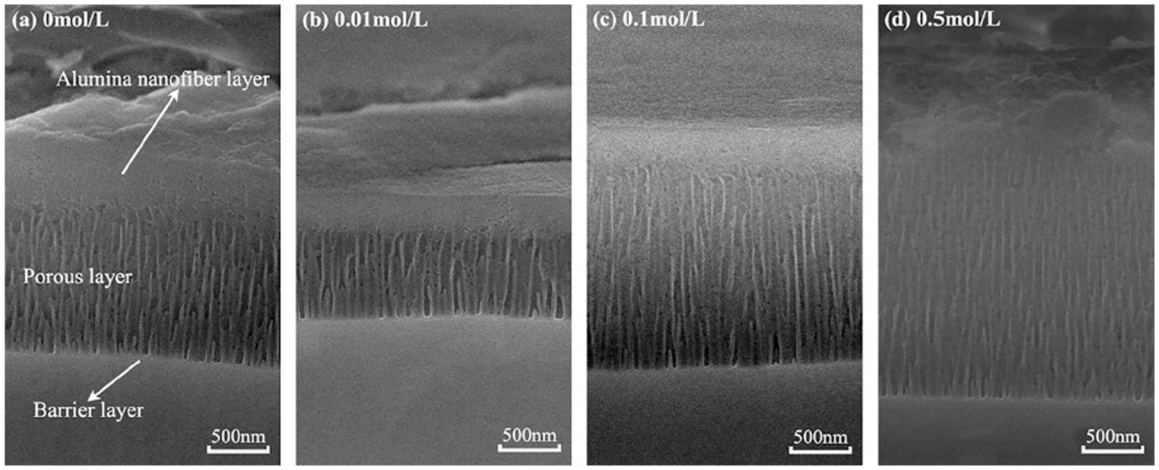

Fig. 10. Cross-sectional SEM images of superhydrophilic anodic oxide films with the smallest contact angle prepared in pyrophosphoric acid solutions with different concentrations of Na_2MoO_4 (0–0.5 mol/L). *Reprinted with permission from the publication by J. Lv, Z.-L. Chen, J. Tang, L. Chen, W.-J. Xie, M.-X. Sun and X.-J. Huang, Surf. Coat. Technol. 446 (9) (2022) 128770* [103].

salts were more efficient for promoting the corrosion resistance of AA2024 [105]. In another study, the corrosion resistance of PEO coating prepared by immersion of AA2024 samples in a silicate electrolyte for 15 min at 450 V was improved by post-treatment sealing with an LDH layer loaded with corrosion inhibitors (nitrate, molybdate and vanadate) [106]. The sealing of PEO-coated AA2024 samples was done by immersion in a mixture of $Zn(NO_3)_2{\cdot}6\,H_2O$ and $NaNO_3$ at pH 6.5 for 12 h at 90 °C to form an LDH. Subsequently, LDH-PEO coated AA2024 samples were immersed in $NaNO_3$, $NaVO_3$ or Na_2MoO_4 solutions for 2 h at 50 °C for intercalation of corrosion inhibitors. Regarding corrosion protection, PEO sealed with LDHs filled with nitrate was somewhat superior to vanadate and molybdate, which is related to the difference in loaded concentrations. The latter is much less for molybdate than for vanadate, as proved by the EDS analysis at the coating surface. In all cases, inhibitor-loaded LDH sealing improved the corrosion performance of bare substrate [106].

6. Molybdate in pre- and post-treatments

This section explores the use of molybdate as a corrosion inhibitor in various pre- and post-treatments.

Chemical pre-treatment is carried out after, or in place of, mechanical pre-treatment to remove surface contamination originating from mechanical pre-treatment and remove oxides present at the metal surface before deposition of protective layers or coatings. [107]. Acid pre-treatment was usually combined with chromic acid (H_2CrO_4 formed when added CrO_3 reacts with water) to induce additional protection. To replace harmful chromic acid, a more environmentally friendly acidic treatment considered combining nitric acid with molybdenum trioxide MoO_3 [108]. The combination of alkaline etching and acid treatment in HNO_3 and MoO_3 resulted in increased pitting resistance of AA1015 when subsequently immersed in chloride solution for up to 1 week.

Anodisation treatment in Na_2MoO_4 solution was used to increase the corrosion resistance of cerium conversion coatings (CeCCs), as shown by Brunelli et al. [109]. CeCCs were deposited on AA5083 in a conversion bath containing $Ce(NO_3)_3$ or $CeCl_3$ in the presence of hydrogen peroxide. CeCC deposited from nitrate solution was thinner and less protective than CeCC deposited from chloride solution. Consecutive deposition from nitrate and chloride solutions produced better results, further improved by anodic polarisation in molybdate solution, leading to a broad passivation range with low current densities in 1% NaCl solution [109].

7. Molybdate conversion coatings

Conversion coatings are a vital way of assuring the adhesion of organic top layers and corrosion protection of underlying substrates. Chemical conversion coatings are formed by immersion of a metal in which the surface is turned into a thin adhering coating by a spontaneous deposition. The immersion solution contains a soluble salt of bearing metal component that precipitates spontaneously on the substrate surface to form a slightly soluble or insoluble metal oxide and/or hydroxide called a conversion coating. The precipitation occurs at the pH at which this process is thermodynamically feasible; thus, the formation of conversion coating is a pH-dependent process. On aluminium alloys, the deposition starts at the intermetallic particles, which are electrochemically more noble with respect to the surrounding matrix and where oxygen reduction takes place, leading to alkanisation required for the deposition of the conversion coating. Deposition then spreads throughout the metal surface [5,110,111]. The thickness of conversion coatings on aluminium alloys ranges between several tens of nanometres at the matrix up to micrometre range at IMPs [5].

Today, the main types of commercialised conversion coatings on aluminium alloys are zirconium- and titanium-oxide-based coatings [5]. Rare earth coatings based on cerium, lanthanum and other rare earth metals have been explored for several decades but have not yet been commercialised. Viable options for conversion coatings are also molybdate conversion coatings (MoCCs). Patents on baths containing molybdic acids or a molybdate were reported in 1939 for protection of zinc and galvanised surfaces, recommending neutral or slightly acid baths containing a buffer agent (e.g. sodium acetate) [112]. Later patents proposed using a molybdate precursor, an activator, usually fluorine-based (e.g. NaF, K_2ZrF_6, H_2ZrF_6), and other additives [113,114]. While Zr- and Ti-based conversion coatings are usually produced at acidic pHs [5], MoCCs have been produced in acid or alkaline conversion baths.[8] Compared to Zn substrates [10,115,116], studies on MoCCs on Al-based substrates have been more scarce.

Roeper et al. tested several compounds as candidates for conversion coatings, selecting molybdate as a promising option together with K_2ZrF_6 and nitric acid as the main constituents of the conversion bath of pH 1.2–2 [117]. The two-step nitric acid activation process yielded more protective coating than the fluoride-activated process and produced protective MoCC on depleted uranium−0.75 wt% titanium alloy [117]. On aluminium alloy 2024-T6, coatings were made using varying amounts of cyanide, fluoride, molybdate and titanium dioxide [118]. A blue coating was optimised to reduce the number of pits on AA2024-T6 in 0.05 M NaCl solution. A cracked mud pattern of the coating was similar to that seen with a chromium conversion coating [118]. This relatively thick coating consisted of various Mo species, including MoO_2, Mo_2O_5, MoO_4^{2-} and MoO_3, with Mo(VI) and Mo(V) being predominantly in the outer part and Mo(IV) in the inner part of the coating [119,120].

A quick method was proposed for the MoCC treatment of Al foil, only 40 μm thick, consisting of immersion in a conversion bath for 1 min at 40 °C. After immersion of Al foil in the bath of H_3PO_4, $(NH_4)_6Mo_7O_{24}{\cdot}4\,H_2O$, NaF, the coating consisted of MoO_3, $(MoO_3)_x(\text{-}P_2O_5)_y$ and $Al_2(MoO_4)_3$ [121]. This composition confirms the synergistic action of molybdate and phosphate ions. MoCCs deposited on Al foil were explored in two other interesting applications. Al foil for packaging of lithium-ion battery (LIB) was protected by MoCC prepared in a bath of $(NH_4)_6Mo_7O_{24}$, NaF, tartaric acid and H_3PO_4 at 50 °C for immersion times between 30 s and 150 s followed by drying at 60 °C [122]. The coatings increased the corrosion resistance in 1 M $LiPF_6$ mixture solvent but also led to a significant increase in adhesion (T-peeling) strength between Al foil and MoCC coating due to chemical coordination and mechanical interlocking (Fig. 11) [122].

Another application in LIBs concerns the protection of aluminium current collector (AlCC), which can corrode in commercial lithium hexafluorophosphate ($LiPF_6$)-esters electrolytes used in LIBs [123]. Namely, during the operation of commercial batteries, trace amounts of water are inevitable, inducing $LiPF_6$ hydrolysis to generate HF and thus corroding AlCC. However, corrosion protection must not jeopardise the conductivity of the AlCC surface when incorporated in LIB. MoCC treatment of AlCC (immersion for 1 min at 40 °C in a bath of H_3PO_4, $(NH_4)_6Mo_7O_{24}{\cdot}4\,H_2O$ and NaF) resulted in passivation of the surface and, at the same time, remaining conductive [123]. A similar demand for corrosion protection with simultaneous electrical conductivity was requested in applications in the electronic industry. Namely, electric conductive coatings are promising for integrated circuit boards and microelectronic systems; they must comply with electrical conductivity requirements, i.e. low electrical contact resistance (ECR) and high corrosion protection. MoCCs were prepared for 0.5 − 6 min at 30 °C in a conversion bath consisting of H_2TiF_6, $(NH_4)_2MoO_4$ with the addition of tannic acid, $KMnO_4$ and $NaVO_3$ [124]. MoCCs exhibited outstanding electrical conductivity and corrosion stability in chloride solution. After immersion in a conversion bath, Al^{3+} and Mg^{2+} dissolved; snowflake-like crystals began to nucleate from the reduction of MoO_4^{2-} and MnO_4^- on the active sites and then interlaced each other to form a crack-free coating. The coating deposited on AA6063 consisted of

[8] The values of pH were stated when available; however, in several papers, the pH was not stated.

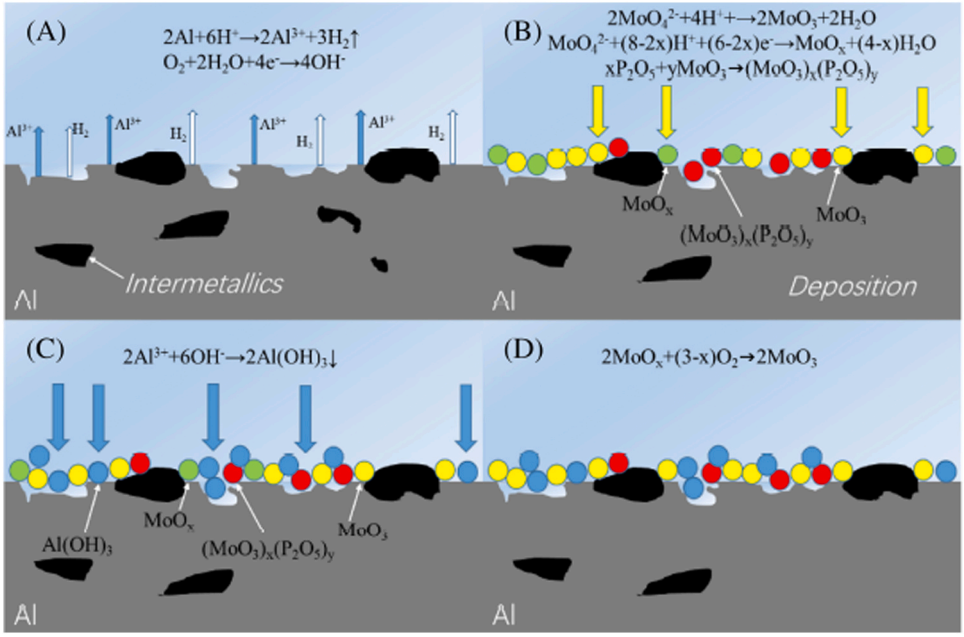

Fig. 11. Schematic diagram of the growth process of Mo conversion coating: (A) dissolution of Al matrix, (B) growth of Mo coating, (C) deposition of Al $(OH)_3$, and (D) oxidation of MoO_x. *Reprinted with permission from the publication by X. Chen and S. Xu, Surf. Interface Anal. 53 (8) (2021) 1048 – 1058* [122].

chemically stable multivalent oxides (MnO, Mn_2O_3, Mn_3O_4, MnO_2, MoO_3, MoO_2, MoO_x) with metallic or semi-metallic states [124].

Alkaline-based treatments were also reported. The effect of surface pre-treatment of AA6061-T6 covered with 10% Al_2O_3 on the preparation and properties of MoCC at pH 7 and 9 was investigated [125]. Treatment at pH 9 was too aggressive for an Al-based substrate, and the conversion process did not produce an efficient coating. The preparation of MoCCs for 3 h at pH 7 on the sample previously alkaline-pickled and oxide-thickened in boiling water produced a coating able to withstand corrosion during 60 days of immersion in 3.5 M NaCl [125]. The importance of oxide thickening at elevated temperatures before conversion treatment in an alkaline molybdate bath was emphasised in [113]. In addition to molybdate, the conversion bath at pH 7–12 may further comprise lithium nitrate, sodium nitrate, ammonia nitrate and combinations thereof, and potassium hexafluorozirconate or potassium hexafluorotitanate [113], as well as post-treatment using calcium hydroxide or other alkali metal salts.

Huang et al. prepared MoCCs under alkaline conditions in a conversion bath of Na_2MoO_4, NaF, sodium citrate and borate at pH = 11 [126]. After 10 min, the coatings deposited on AA6063 were more than 30 μm thick and were not cracked. The conversion process was ascribed to the following reactions [126]:

$$MoO_4^{2-} + 2\,H_2O \rightarrow MoO_3{\cdot}H_2O + 2\,OH^- \quad (19)$$

$$3MoO_4^{2-} + 2Al + 6\,H^+ \rightarrow 3\,H_2 + Al_2(MoO_4)_3\downarrow \quad (20)$$

$$2Al + 6\,F^- + 6\,H_2O \rightarrow 3\,H_2 + 2AlF_3\downarrow + 6\,OH^- \quad (21)$$

The first step in the coating formation is the dissolution of Al as AlO_2^- consuming hydroxyl ions. The subsequent decrease in pH leads to the precipitation of Al, Mo and Al/Mo oxides, which effectively protect the underlying alloy [126].

In addition to protecting individual alloys, the deposition of conversion coating on multiple metals in contact is important, e.g., in an automobile body. Kosaba et al. investigated the possibility of protecting galvanically connected Al alloy-steel joints (AA5083 and AISI 1045 carbon steel) using MoCCs prepared in a conversion bath of Na_2MoO_4 at pH 8–12 and assisted by potentiostatic oxidation [127]. The Mo coatings suppressed the cathodic activity of Al_6(Fe,Mn) particles, resulting in lowering galvanic activity measured in dilute synthetic seawater [127].

8. Concluding remarks and critical assessment

Molybdate has been recognised as an inhibitor of corrosion of aluminium alloys, zinc, and steel for over 80 years (Fig. 4). It has been considered a potential chromate replacement for several decades since it is non-toxic and comparatively efficient under appropriate conditions. Its efficient inhibition of corrosion is based on reducing aqueous molybdate species to slightly soluble molybdenum oxides at the metal surface. Reduced oxides have a mixed valency ranging from (IV) to (V) and are slightly soluble or insoluble (Fig. 8). Molybdate is exceptionally efficient against pitting corrosion, shifting the pitting potential for several hundred millivolts in the positive direction; however, only when added at sufficiently high concentrations of 100 ppm and higher. Reduced oxide can be subsequently oxidised and polymerised (Fig. 8); these processes are based on rich molybdenum chemistry and the ability to form polynuclear species. In addition to pitting corrosion, molybdate was reported to efficiently reduce galvanic corrosion and environmental fatigue cracking and even help repassivation after damage. The inhibitive action of molybdate is only under aerated conditions; namely, it is a weak oxidant in contrast to chromate. Although it is predominantly an anodic inhibitor, it also retards the oxygen reduction reaction. For aluminium alloy substrates, it is generally established that the intermetallic particles act as primary sites of molybdate deposition at the surface, and the efficiency of protection depends on the alloy type. Despite valuable research studied hitherto performed on Al and Al alloys as summarised in Fig. 8, details on the general Mo chemistry and inhibition mechanism remain to be revealed entirely.

First, the relationship between aqueous Mo speciation chemistry and pH-dependent deposition of Mo species is crucial for optimising the deposition process. However, no systematic study has been performed in this regard. Second, identifying Mo species of mixed valency and polymerised Mo species deserves more attention. In this regard, Raman and XPS analyses have been used in recent studies [37,51] which brought about a significant improvement compared to the studies from the 1990's. However, using a technique such as Time-of-flight secondary ion mass spectrometry (ToF-SIMS), which can identify mono- and polynuclear species, would be beneficial for describing the mechanism more

precisely. Further, a more intensive introduction of local techniques such as scanning Kelvin probe microscopy (SKPFM) and scanning vibrating electrode technique (SVET) would elucidate the details of inhibition mechanisms considering the change in local electrochemical and chemical activities.

Third, when using Mo as an inhibitor for Al alloys's corrosion, further improvement is required regarding the systematic study of the relationship between the composition and type of IMPs and conditions for the precipitation and reduction of Mo species.

Fourth, introducing calculation and molecular simulation methods based on density functional theory (DFT) and molecular dynamics (MD) would largely contribute to understanding the adsorption mechanism of molybdate anions on the Al surface and the anion-surface interactions. Some quantum chemical parameters of inorganic inhibitors were compared with experimental results [128]. On steel surfaces, several studies have dealt with such issues [129,130] but no similar study exists on the Al alloys.

Besides being an aqueous inhibitor, molybdate is very efficient as an inhibitor in cooling systems where water is mixed with alcohol. However, only a few studies have regarded this critical issue, especially in light of the further intensive development of the transportation industry and the need for a detailed understanding of the corrosion mechanism of Al alloys at elevated temperatures in non-aqueous media.

Molybdate can also be added to anodised baths to reduce corrosion during anodisation in acidic and alkaline media. Using molybdate as a pre- and post-treatment or sealing application should be intensified by introducing non-toxic inhibitors.

The great potential of molybdate is its ability to act synergistically with different anions and cations, which should be further explored in sustainable corrosion inhibition based on the interaction of existing chemical compounds. Recent literature reports encouraging results on the applications of molybdate conversion coatings in electronic industries and batteries; however, systematic research on different alloys is missing, as well as the elucidation of the relationship between deposition bath parameters and properties of the MoCCs. Finally, the possibility of encapsulating into various coatings and adding the prolonged inhibitive action or using molybdate-based pre- or post-treatments rounds off molybdate's wide range of applications in corrosion science and should be explored further.

Funding

The author acknowledges the financial support from the Slovenian Research and Innovation Agency (research core funding No. P2–0393).

Declaration of Competing Interest

The author declares that she has no known competing financial interests or personal relationships that could have appeared to influence the work reported in this paper.

Data availability

No data was used for the research described in the article.

Acknowledgements

The author thanks her colleagues Prof. Anton Kokalj, for drawing tetravalent molybdate ion in the *XCrysDen* programme (Fig. 2a), Dr. Matic Lozinšek for data on Mo-O bonds, Ana Kraš, MSc, and Tjaša Pavlovčič, MSc, for drawing and calculating the fraction diagram of molybdenum species in the Spana programme (Fig. 3), and Dr. Peter Rodič for critical reading of the manuscript.

References

[1] M. Kendig, R.G. Buchheit, Corrosion Inhibition of aluminum and aluminum alloys by soluble chromates, chromate coatings, and chromate-free coatings, CORROSION 59 (5) (2003) 379–400, https://doi.org/10.5006/1.3277570.
[2] B.R.W. Hinton, Corrosion prevention and chromates: the end of an era? Met. Finish. 89/9 (1991) 55–61.
[3] B.R.W. Hinton, Corrosion prevention and chromates: the end of an era? Met. Finish. 89/10 (1991) 15–20.
[4] O. Gharbi, S. Thomas, C. Smith, N. Birbilis, npj Mater. Degrad. 2 (2018) 12, https://doi.org/10.1038/s41529-018-0034-5.
[5] I. Milošev, G.S. Frankel, Review—Conversion coatings based on zirconium and/or titanium, J. Electrochem. Soc. 165 (3) (2018) C127–C144, https://doi.org/10.1149/2.0371803jes.
[6] F. Peltier, D. Thierry, Review of Cr-free coatings for the corrosion protection of aluminum aerospace alloys, Coatings 12 (2022) 518, https://doi.org/10.3390/coatings12040518.
[7] R.L. Twite, G.P. Bierwagen, Reviews of alternatives to chromate for corrosion protection of aluminum aerospace alloys, Prog. Org. Coat. 33 (2) (1998) 91–100, https://doi.org/10.1016/S0300-9440(98)00015-0.
[8] M.S. Vukasovich, J.P.G. Farr, Molybdate in corrosion inhibition—a review, Polyhedron 5 (1-2) (1986) 551–559, https://doi.org/10.1016/S0277-5387(00)84963-3.
[9] V. Anitha Kumari, K. Sreevalsan, S.M.A. Shibli, Sodium molybdate for the effective protection of steel: a comprehensive review, Corros. Prev. Contr. 48 (3) (2001) 83–109.
[10] D.E. Walker, G.D. Wilcox, Molybdate based conversion coatings for zinc and zinc alloy surfaces: a review, Trans. Inst. Met. Finish. 86 (5) (2008) 251–259, https://doi.org/10.1179/174591908X345022.
[11] L. Wang, G.-H. Zhang, J. Dang, K.-C. Chou, Oxidation roasting of molybdenite concentrate, Trans. Nonferrous Met. Soc. China 25 (2015) 4167–4174, https://doi.org/10.1016/S1003-6326(15)64067-5.
[12] M. Pourbaix, Atlas of Electrochemical Equilibria in Aqueous Solution, 2nd ed., NACE, Cebelcor, Houston, TX, Brussels (1974).
[13] I. Filipović, S. Lipanović, Opća i anorganska kemija (in Croatian), Školska knjiga, Zagreb (1982).
[14] V. Maurice, P. Marcus, Molybdenum effects on the stability of passive films unraveled at the nanometer and atomic scales, npj Mater. Degrad. 8 (2024) 3, https://doi.org/10.1038/s41529-023-00418-6.
[15] J.-P. Jovilet, Metal Oxide Nanostructures Chemistry. Synthesis from Aqueous Solutions, 2nd ed., Oxford University Press, New York, USA (2015).
[16] A. Kokalj, XCrySDen—a new program for displaying crystalline structures and electron densities, J. Mol. Graph. Model. 17 (1999) 176–179. Code available from http://www.xcrysden.org/.
[17] A.D. Fortes, Crystal structures of deuterated sodium molybdate dihydrate and sodium tungstate dihydrate from time-of-flight neutron powder diffraction, E Crystallogr. Commun. 71 (7) (2015) 799–806, https://doi.org/10.1107/S2056989015011354.
[18] A.D. Fortes, Crystal structures of spinel-type Na_2MoO_4 and Na_2WO_4 revisited using neutron powder diffraction, E Crystallogr. Commun. 71 (6) (2015) 592–596, https://doi.org/10.1107/S2056989015008774.
[19] I. Puigdomènech, (2020), Spana https://sites.google.com/site/chemdiagr/home/java-versions.
[20] I. Puigdomènech, E. Colàs, M. Grivé, I. Campos, and D. García, MRC Online Proc. Libr. 111 (2014) 111. https://link.springer.com/article/10.1557/opl.2014.635.
[21] P.L. Smedley, D.G. Kinniburgh, Molybdenum in natural waters: a review of occurrence, distributions and controls, Appl. Geochem. 84 (2017) 387–432, https://doi.org/10.1016/j.apgeochem.2017.05.008.
[22] P. Gouzerh, M. Che, From Scheele and Berzelius to Müller: Polyoxometalates (POMs) revisited and the "missing link" between the bottom up and top down approaches, L'Actualité Chim. 298 (2006) 9–22, https://new.societechimiquedefrance.fr/numero/de-scheele-et-berzelius-a-muller-les-polyoxometallates-poms-revisites-et-le-chainon-manquant-entre-les-approches-bottom-up-et-top-down-p9-n298/.
[23] H.-J. Lunk, H. Harti, The fascinating polyoxometalates, ChemTexts 7 (2021) 26, https://doi.org/10.1007/s40828-021-00145-y.
[24] IARC Monographs on the Evaluation of Carcinogenic Risks to Humans, vol. 118: Welding, Molybdenum trioxide, and Indium Tin Oxide, International Agency for Research on Cancer, Lyon, France (2018).
[25] https://monographs.iarc.who.int/wp-content/uploads/2018/06/mono100C-9.pdf.
[26] https://www.osha.gov/sites/default/files/publications/OSHA3844.pdf.
[27] ThermoFisher Safety Data Sheet Sodium-molybdate-dihydrate.
[28] ThermoFisher Safety Data Sodium dichromate.
[29] ThermoFisher Safety Data Sheet Sodium Chromate.
[30] A.L. Bayes, Noncorrosive antifreeze liquid, U.S. Patent 2,147,395 (1939), https://patents.google.com/patent/US2147395.
[31] R. Parks Langguth, E. Seifter, Corrosion-inhibited liquid fertilizer compositions, U.S. Patent 3,024,100 (1962), https://patents.google.com/patent/US3024100A/en.
[32] W.C. Moshier, G.D. Davis, Interaction of molybdate anions with the passive film on aluminum, CORROSION 46 (1) (1990) 43–50, https://doi.org/10.5006/1.3585065.
[33] K.C. Emergül, A.A. Aksüt, The effect of sodium molybdate on the pitting corrosion of aluminium, Corros. Sci. 45 (11) (2003) 2415–2433, https://doi.org/10.1016/S0010-938X(03)00097-0.

[34] S. Zein El Abedin, Role of chromate, molybdate and tungstate anions on the inhibition of aluminium in chloride solutions, J. Appl. Electrochem 31 (6) (2001) 711–718, https://doi.org/10.1023/A:1017587911095.
[35] C.B. Breslin, G. Treacy, W.M. Carroll, Studies on the passivation of aluminium in chromate and molybdate solutions, Corros. Sci. 36 (7) (1994) 1143–1154, https://doi.org/10.1016/0010-938X(94)90139-2.
[36] C.N. Panagopoulos, E.P. Georgious, A.G. Gavras, Corrosion and wear of 6082 aluminum alloy, Tribol. Int. 42 (6) (2009) 886–889, https://doi.org/10.1016/j.triboint.2008.12.002.
[37] O. Lopez-Garrity, G.S. Frankel, Corrosion inhibition of aluminum alloy 2024-T3 by sodium molybdate, J. Electrochem. Soc. 161 (3) (2014) C95–C106, https://doi.org/10.1149/2.044403jes.
[38] D. Wang, M. Wu, J. Ming, J. Shi, Inhibitive effect of sodium molybdate on corrosion behaviour of AA6061 aluminium alloy in simulated concrete pore solutions, Constr. Build. Mater. 270 (2) (2021) 121463, https://doi.org/10.1016/j.conbuildmat.2020.121463.
[39] M.A. Jakab, F. Presuel-Moreno, J.R. Scully, Critical concentrations associated with cobalt, cerium, and molybdenum inhibition of AA2024-T3 corrosion: Delivery from Al-Co-Ce(-Mo) alloys, CORROSION 61 (3) (2005) 246–263, https://doi.org/10.5006/1.3280634.
[40] F.J. Presuel-Morreno, M.A. Jakab, J.R. Scully, Inhibition of the oxygen reduction reaction on copper with cobalt, cerium, and molybdate ions, J. Electrochem. Soc. 152 (9) (2005). B376-B387, https://iopscience.iop.org/article/10.1149/1.1997165.
[41] M.A. Jakab, F.J. Presuel-Morreno, J.R. Scully, Effect of molybdate, cerium, and cobalt ions on the oxygen reduction reaction on AA2024-T3 and selected intermetallics. Experimental and modeling studies, J. Electrochem. Soc. 153 (7) (2006). B244-B252, https://iopscience.iop.org/article/10.1149/1.2200300.
[42] A.M. Shams El Din, L. Wang, Mechanism of corrosion inhibition by sodium molybdate, Desalination 107 (1) (1996) 29–43, https://doi.org/10.1016/0011-9164(96)00148-8.
[43] M.A. Stranick, The corrosion inhibition of metals by molybdate Part I. Mild steel, CORROSION 40 (6) (1984) 296–302, https://doi.org/10.5006/1.3581956.
[44] M.J. Pryor, M. Cohen, The inhibition of the corrosion of iron by some anodic inhibitors, J. Electrochem. Soc. 100 (5) (1953) 203–215, https://iopscience.iop.org/article/10.1149/1.2781106.
[45] W.D. Robertson, Molybdate and tungstate as corrosion inhibitors and the mechanism of inhibition, J. Electrochem. Soc. 98 (3) (1951) 94–100, https://iopscience.iop.org/article/10.1149/1.2778118.
[46] W.A. Badawy, F.M. Al-Kharafi, The inhibition of the corrosion of Al, Al-6061 and Al-Cu in chloride free aqueous media: I. Passivation in acidic solution, Corros. Sci. 39 (4) (1997) 681–700, https://doi.org/10.1016/S0010-938X(97)89336-5.
[47] W.A. Badawy, F.M. Al-Kharafi, A.S. El-Azab, Electrochemical behaviour and corrosion inhibition of Al, Al-6061 and Al-Cu in neutral aqueous solutions, Corros. Sci. 41 (4) (1999) 709–727, https://doi.org/10.1016/S0010-938X(98)00145-0.
[48] F.M. Al-Kharafi, W.A. Badawy, Inhibition of corrosion of Al-6061, aluminium, and an aluminium-copper alloy in chloride-free aqueous media: Part 2- Behavior in basic solutions, CORROSION 54 (5) (1998) 377–385, https://doi.org/10.5006/1.3284865.
[49] P.M. Natishan, E. McCafferty, G.K. Hubler, The effect of pH of zero charge on the pitting potential, J. Electrochem. Soc. 133 (5) (1986) 1061–1062, https://iopscience.iop.org/article/10.1149/1.2108708/pdf.
[50] C. Monticelli, G. Brunoro, A. Frignani, G. Trabanelli, Evaluation of corrosion inhibitors by electrochemical noise analysis, J. Electrochem. Soc. 139 (3) (1992) 706–711, https://iopscience.iop.org/article/10.1149/1.2069288.
[51] D.S. Kharitonov, I. Dobryden, B. Sefer, J. Ryl, A. Wrzesińska, I.V. Makarova, I. Bobowska, I.I. Kurilo, P.M. Claesson, Surface and corrosion properties of AA6063-T5 aluminum alloy in molybdate-containing sodium chloride solutions, Corros. Sci. 171 (7) (2020) 108658, https://doi.org/10.1016/j.corsci.2020.108658.
[52] J.W.J. Silva, E.N. Codaro, R.Z. Nakazato, L.R.O. Hein, Influence of chromate, molybdate and tungstate on pit formation in chloride medium, Appl. Surf. Sci. 252 (11) (2005) 1117–1122, https://doi.org/10.1016/j.apsusc.2005.02.030.
[53] R. Salghi, L. Bazzi, B. Hammouti, A. Bendou, E. Ait Addi, S. Kertit, Comparative study of the effect of inorganic ions on the corrosion of Al 3003 and 6063 in carbonate solution, Prog. Org. Coat. 51 (2) (2004) 113–117, https://doi.org/10.1016/j.porgcoat.2004.06.004.
[54] H.H. Uhlig, P.F. King, The Flade potential of iron passivated by various inorganic corrosion inhibitors, J. Electrochem. Soc. 106 (1) (1959) 1–7, https://iopscience.iop.org/article/10.1149/1.2427255.
[55] R.C. McCune, R.L. Shilts, S.M. Ferguson, A study of film formation on aluminium in aqueous solutions using rutherford backscattering spectroscopy, Corros. Sci. 22 (11) (1982) 1049–1065, https://doi.org/10.1016/0010-938X(82)90091-9.
[56] A.Kh Bairamov, S. Zakipor, C. Leygraph, An XPS investigation of dichromate and molybdate inhibitors on aluminium, Corros. Sci. 25 (1) (1985) 69–73, https://doi.org/10.1016/0010-938X(85)90089-7.
[57] T.H. Nguyen, R.T. Foley, On the mechanism of pitting of aluminium, J. Electrochem. Soc. 126 (11) (1979) 1855–1860, https://iopscience.iop.org/article/10.1149/1.2128815.
[58] J.S. Warner, R.P. Gangloff, Molybdate inhibition of corrosion fatigue crack propagation in precipitation hardened Al–Cu–Li, Corros. Sci. 62 (9) (2012) 11–21, https://doi.org/10.1016/j.corsci.2012.03.038.
[59] S.E. Gaylon Dorman, T.A. Reid, B.K. Hoff, D.H. Henning, S.E. Collins, The effect of corrosion inhibitors on environmental fatigue crack growth in Al–Zn–Mg–Cu, Eng. Fract. Mech. 137 (3) (2015) 56–63, https://doi.org/10.1016/j.engfracmech.2014.12.009.
[60] S.B. Madden, D.J. Moosbauer, J.R. Scully, Effects of chromate and molybdate ions on scratch repassivation behavior of precipitation hardened aluminum alloys, ECS Trans. 50 (30) (2013) 57–78, https://iopscience.iop.org/article/10.1149/05030.0057ecst.
[61] B.D. Chambers, S.R. Taylor, M.W. Kendig, Rapid discovery of corrosion inhibitors and synergistic combinations using high-throughput screening methods, CORROSION 61 (5) (2005) 480–489, https://doi.org/10.5006/1.3280648.
[62] B.D. Chambers, S.R. Taylor, High-throughput assessment of inhibitor synergies on aluminium alloy 2024-T3 through measurement of surface copper enrichment, CORROSION 63 (3) (2007) 268–276, https://doi.org/10.5006/1.3278353.
[63] B.D. Chambers, S.R. Taylor, The high throughput assessment of aluminium alloy corrosion using fluorometric methods. Part II – a combinatorial study of corrosion inhibitors and synergistic combinations, Corros. Sci. 49 (3) (2007) 1597–1609, https://doi.org/10.1016/j.corsci.2006.08.006.
[64] S.R. Taylor, B.D. Chambers, Identification and characterization of nonchromate corrosion inhibitor synergies using high-throughput methods, CORROSION 64 (3) (2008) 255–270, https://doi.org/10.5006/1.3278470.
[65] O. Lopez-Garrity, G.S. Frankel, Synergistic corrosion inhibition of AA2024-T3 by sodium silicate and sodium molybdate J, Electrochem. Soc. Lett. 3 (10) (2014). C33-C35, https://iopscience.iop.org/article/10.1149/2.0021410eel.
[66] X. Li, S. Deng, H. Fu, Sodium molybdate as a corrosion inhibitor for aluminium in H_3PO_4 solution, Corros. Sci. 53 (9) (2011) 2748–2753, https://doi.org/10.1016/j.corsci.2011.05.002.
[67] D. Saran, A. Kumar, S. Bathula, S. Klaumünzer, K.K. Sahu, Review on the phosphate-based conversion coatings of magnesium and its alloys, Int. J. Miner. Met. 29 (7) (2022) 1435–1452, https://doi.org/10.1007/s12613-022-2419-2.
[68] X.F. Liu, S.J. Huang, H.C. Gu, Corrosion protection of an aluminum alloy with nontoxic compound inhibitors in chloride media, CORROSION 58 (10) (2002) 826–834, https://doi.org/10.5006/1.3287664.
[69] D. Quan Zhang, X. Jin, B. Xie, H. Goun Joo, L. Xin Gao, K. Yong Lee, Corrosion inhibition of ammonium molybdate for AA6061 alloy in NaCl solution and its synergistic effect with calcium gluconate, Surf. Inter. Anal. 44 (4) (2012) 78–83, https://doi.org/10.1002/sia.3774.
[70] C.E. Byrne, N.V. Quesada Cangahuala, O. D'Alessandro, C. Deyá, Cerium and aluminum molybdates as inhibitors of the aluminum AA1050 corrosion process in aqueous NaCl solutions, Mater. Corros. 75 (2024) 73–83, https://doi.org/10.1002/maco.202313940.
[71] G.A. Zhang, L.Y. Xu, Y.F. Cheng, Mechanistic aspects of electrochemical corrosion of aluminum alloy in ethylene glycol–water solution, Electrochim. Acta 53 (2008) 8245–8252, https://doi.org/10.1016/j.electacta.2008.06.043.
[72] M. Asadikiya, M. Ghorbani, Effect of inhibitors on the corrosion of automotive aluminum alloy in ethylene glycol-water mixture, CORROSION 67 (12) (2011) 126001-1–126001-5, https://doi.org/10.5006/1.3666860.
[73] Y. Liu, Y.F. Cheng, Inhibition of corrosion of 3003 aluminum alloy in ethylene glycol-water solutions, J. Mat. Eng. Perf. 20 (6) (2011) 271–275, https://link.springer.com/article/10.1007/s11665-010-9684-3.
[74] C. Monticceli, G. Brunoro, F. Zucchi, F. Fagioli, Inhibition of localized attack on the aluminium alloy AA6351 in glycol/water solutions, Werkst. Korros. 40 (6) (1989) 393–398, https://doi.org/10.1002/maco.19890400607.
[75] K.P. Fivizzani, Use of molybdate as a cooling water corrosion inhibitor at higher temperatures, US Patent 5,192,447 (1993), https://patents.google.com/patent/US5192447A/en.
[76] J.J. Velasco, M. Ardanuy, M. Antunes, Layer double hydroxide (LDHs) as functional fillers in polymer nanocomposites", chapter 4 In: Advances in Polymer Nanocomposites. Types and Applications", ed. F. Gao, Woodhead Publishing Series in Composites Science and Engineering (2012) 91–130.
[77] A. Sharma, S. Kumari, S. Sharma, T. Singh, S. Kumar, A. Thakur, S.K. Bhatia, A.K. Sharma, Layered double hydroxides: an insight into the role of hydrocalcite-type anion clays in energy and environmental applications with current progress and recent prospects, 22 (6) (2023), 100399, https://doi.org/10.1016/j.mtsust.2023.100399.
[78] R.G. Buchheit, H. Guan, S. Kahajanam, F. Wong, Active corrosion protection and corrosion sensing in chromate-free organic coatings, Prog. Org. Coat. 47 (3-4) (2003) 174–182, https://doi.org/10.1016/j.porgcoat.2003.08.003.
[79] Y. Zhang, J. Liu, Y. Li, M. Yu, S.M. Li, B. Xue, Fabrication of inhibitor anion-intercalated layered double hydroxide host films on aluminum alloy 2024 and their anticorrosion properties, J. Coat. Tehnol. Res. 12 (2) (2015) 293–302, https://doi.org/10.1007/s11998-014-9644-1.
[80] M.F. Montemor, D.V. Snihirova, M.G. Taryba, S.V. Lamaka, I.A. Kartsonakis, A. C. Balasks, G.C. Kordas, J. Tedim, A. Kuznetsova, M.L. Zheludkevich, M.D. S. Ferreira, Evaluation of self-healing ability in protective coatings modified with combinations of layered double hydroxides and cerium molibdate nanocontainers filled with corrosion inhibitors, Electrochim. Acta 60 (1) (2012) 31–40, https://doi.org/10.1016/j.electacta.2011.10.078.
[81] Y. Zhang, P. Yu, J. Wu, F. Chen, Y. Li, Y. Zhang, Y. Zuo, Y. Qi, Enhancement of anticorrosion protection via inhibitor-loaded ZnAlCe-LDH nanocontainers embedded in sol–gel coatings, J. Coat. Technol. Res. 15 (2) (2018) 303–313, https://link.springer.com/article/10.1007/s11998-017-9978-6.
[82] R. Subasri, K.R.C. Soma Raju, D.S. Reddy, A. Jyothirmayi, V.S. Ijeri, O. Prakash, S. P. Gaydos, Environmentally friendly Zn–Al layered double hydroxide (LDH)-based sol–gel corrosion protection coatings on AA 2024-T3, J. Coat. Res. Technol. 16 (5) (2019) 1447–1463, https://link.springer.com/article/10.1007/s11998-019-00229-y.

[83] I. Imanieh, A. Asfhar, Corrosion protection of aluminum by smart coatings containing layered double hydroxide (LDH) nanocontainers, J. Mater. Res. Technol. 8 (3) (2019) 3004–3023, https://doi.org/10.1016/j.jmrt.2018.05.030.

[84] E.V. Bendinelli, A.C. Rocha, O.E. Barcia, I.V. Aoki, I.C.P. Margarit-Mattos, Effects of lamellar reconstruction routes in the release of molybdate encapsulated in Mg-Al layer double hydroxides, Mater. Chem. Phys. 173 (4) (2016) 26–32, https://doi.org/10.1016/j.matchemphys.2015.12.049.

[85] K.A. Yasakau, J. Tedim, M.L. Zheludkevich, R. Drumm, M. Sheh, M. Wittmar, M. Veith, M.G.S. Ferreira, Cerium molybdate nanowires for active corrosion protection of aluminium alloys, Corros. Sci. 58 (5) (2012) 41–51, https://doi.org/10.1016/j.corsci.2012.01.012.

[86] K.A. Yasakau, J.S. Kallip, M.L. Zheludkevich, M.G.S. Ferreira, Active corrosion protection of AA2024 by sol–gel coatings with cerium molybdate nanowires, Electrochim. Acta 112 (12) (2013) 236–246, https://doi.org/10.1016/j.electacta.2013.08.126.

[87] K.A. Yasakau, J. Tedim, M.F. Montemor, A.N. Salak, M.L. Zheludkevich, M.G. S. Ferreira, Mechanisms of localized corrosion inhibition of AA2024 by cerium molybdate nanowires, J. Phys. Chem. C 117 (2) (2013) 5811–5823, https://doi.org/10.1021/jp3124633.

[88] S.A.S. Dias, S.V. Lamaka, T.C. Diamantino, M.G.S. Ferreira, Synergistic protection against corrosion of AA2024-T3 by sol-gel coating modified with La and Mo-enriched zeolites, J. Electrochem. Soc. 161 (4) (2014) C215-C222, https://iopscience.iop.org/article/10.1149/2.064404jes.

[89] I.A. Kartsonakis, A.C. Balaskas, G.C. Kordas, Influence of cerium molybdate containers on the corrosion performance of epoxy coated aluminium alloys 2024-T3, Corros. Sci. 53 (11) (2011) 3771–3779, https://doi.org/10.1016/j.corsci.2011.07.026.

[90] I.A. Kartsonakis, G. Kordas, Synthesis and characterization of cerium molybdate nanocontainers and their inhibitor complexes, J. Am. Ceram. Soc. 93 (1) (2010) 65–73, https://doi.org/10.1111/j.1551-2916.2009.03310.x.

[91] I.A. Kartsonakis, D.A. Dragatogiannis, E.P. Koumoulos, A. Karantonis, C. A. Charitidis, Corrosion behaviour of dissimilar friction stir welded aluminium alloys reinforced with nanoadditives, Mater. Des. 102 (7) (2016) 56–67, https://doi.org/10.1016/j.matdes.2016.04.027.

[92] V. Moutarlier, B. Neveu, M.P. Gigandet, Evolution of corrosion protection for sol–gel coatings doped with inorganic inhibitors, Surf. Coat. Technol. 202 (10) (2008) 2052–2058, https://doi.org/10.1016/j.surfcoat.2007.08.040.

[93] L. Famiyeh, X. Huang, Plasma electrolytic oxidation coatings on aluminium alloys: microstructure, properties and applications, Mod. Concept Mater. Sci. 2 (1) (2019) 6–13. MCMS.MS.ID.000526.

[94] M. Paz Martinez-Viademonte, S.T. Abrahami, T. Hack, M. Burchardt, H. Terryn, A review on anodizing of aerospace aluminum alloys for corrosion protection, Coatings 10 (11) (2020) 1106, https://doi.org/10.3390/coatings10111106.

[95] V. Moutarlier, M.P. Gigandet, L. Ricq, J. Pagetti, Electrochemical characterisation of anodic oxidation films formed in the presence of corrosion inhibitors, Appl. Surf. Sci. 183 (1-2) (2001) 1–9, https://doi.org/10.1016/S0169-4332(01)00364-6.

[96] V. Moutarlier, M.P. Gigandet, J. Pagetti, L. Ricq, Molybdate/sulfuric acid anodising of 2024-aluminium alloy: influence of inhibitor concentration on film growth and on corrosion resistance, Surf. Coat. Technol. 173 (1) (2003) 87–95, https://doi.org/10.1016/S0257-8972(03)00511-5.

[97] V. Moutarlier, M.P. Gigandet, B. Normand, J. Pagetti, EIS characterisation of anodic films formed on 2024 aluminium alloy, in sulphuric acid containing molybdate or permanganate species, Corros. Sci. 47 (4) (2005) 937–951, https://doi.org/10.1016/j.corsci.2004.06.019.

[98] M. Garćia-Rubio, P. Ocón, A. Climent-Ford, R.W. Smith, M. Curioni, G. E. Thompson, P. Skeldon, A. Lavía, I. Garćia, Influence of molybdate species on the tartaric acid/sulphuric acid anodic films grown on AA2024 T3 aerospace alloy, Corros. Sci. 51 (9) (2009) 2034–2042, https://doi.org/10.1016/j.corsci.2009.05.034.

[99] P. Kwolek, A. Kamiński, K. Dychtoń, M. Drajewicz, J. Sieniawski, The corrosion rate of aluminium in the orthophosphoric acid solutions in the presence of sodium molybdate, Corros. Sci. 106 (5) (2016) 208–216, https://doi.org/10.1016/j.corsci.2016.02.005.

[100] M. Wojnicki, P. Kwolek, Spectrophotometric study of corrosion inhibition of aluminium in orthophosphoric acid aqueous solution using sodium molybdate, Corr. Eng. Sci. Technol. 54 (3) (2019) 199–204, https://doi.org/10.1080/1478422X.2018.1557914.

[101] K. Dychtoń, P. Kwolek, The replacement of chromate by molybdate in phosphoric acid-based etch solutions for aluminium alloy, Corr. Eng. Sci. Technol. 53 (3) (2018) 234–240, https://doi.org/10.1080/1478422X.2018.1446582.

[102] P. Kwolek, Corrosion behaviour of 7075 aluminium alloy in acid solution, RSC Adv. 10 (2020) 26078, https://doi.org/10.1039/D0RA04215C.

[103] J. Lv, Z.-L. Chen, J. Tang, L. Chen, W.-J. Xie, M.-X. Sun, X.-J. Juang, Study on the superhydrophilic modification and enhanced corrosion resistance method of aluminum alloy distillation desalination tubes, Surf. Coat. Technol. 446 (9) (2022) 128770, https://doi.org/10.1016/j.surfcoat.2022.128770.

[104] F. Simchen, M. Sieber, A. Kopp, T. Lampke, Introduction to plasma electrolytic oxidation—an overview of the process and applications, Coatings 10 (7) (2020) 628, https://doi.org/10.3390/coatings10070628.

[105] R. del Olmo, M. Mohedano, P. Visser, E. Matykina, R. Arrabal, Flash-PEO coatings loaded with corrosion inhibitors on AA2024, Surf. Coat. Technol. 402 (11) (2020) 126317, https://doi.org/10.1016/j.surfcoat.2020.126317.

[106] G. Liu, X. Lu, X. Zhang, T. Zhang, F. Wang, Improvement of corrosion resistance of PEO coatings on Al alloy by formation of ZnAl layered double hydroxide, Surf. Coat. Technol. 441 (2022) 128528, https://doi.org/10.1016/j.surfcoat.2022.128528.

[107] U. Tiringer, J. Kovač, I. Milošev, Effects of mechanical and chemical pre-treatments on the morphology and composition of surfaces of aluminium alloys 7075-T6 and 2024-T3, Corros. Sci. 119 (5) (2017) 46–59, https://doi.org/10.1016/j.corsci.2017.02.018.

[108] H. Kakinuma, I. Muto, Y. Oya, T. Momii, Y. Sugawara, N. Hara, Improving the pitting corrosion resistance of AA1050 aluminum by removing intermetallic particles during conversion treatments, Mater. Trans. 62 (8) (2021) 1160–1167, https://doi.org/10.2320/matertrans.MT-M2021071.

[109] K. Brunelli, M. Magrini, M. Dabalá, Method to improve corrosion resistance of AA5083 by cerium based conversion coating and anodic polarisation in molybdate solution, Cor. Eng. Sci. Technol. 47 (3) (2012) 223–232, https://doi.org/10.1179/1743278212Y.0000000001.

[110] I. Milošev, Contemporary modes of corrosion protection and functionalization of materials, Acta Chim. Slov. 66 (3) (2019) 511–533, https://doi.org/10.17344/acsi.2019.5162.

[111] K. Ogle, R.G. Buchheit, Conversion Coatings. chapter 5.3 In: Encyclopaedia of Electrochemistry, Wiley-VCH, 2007, pp. 460–499, https://doi.org/10.1002/9783527610426.bard040503.

[112] Patent GB502360A, "Process for producing coatings on zinc and galvanised articles (1939), https://patents.google.com/patent/GB502360A/en?oq=GB502360+A.

[113] Z. Minevski, J. Maxey, B. Nelson, E. Cahit, Isomolybdate conversion coatings, US Patent 6,432,224 B1 (2002), https://patentimages.storage.googleapis.com/f4/98/b4/63b79053398b23/US6432224.pdf.

[114] D. Chidambaram, D. Rodriguez, Molybdate-based composition and conversion coating, WO Patent 2019113479 A1 (2019), https://patents.google.com/patent/WO2019113479A1/en.

[115] S.V. Oleinik, Yu.I. Kuznetsov, Corrosion inhibitors in coversion coatings, IV, Prot. Met. 43 (4) (2007) 391–397.

[116] A.A.O. Magalhães, I.C.P. Margarit, O.R. Mattos, Molybdate conversion coatings on zinc surfaces, J. Electroanal. Chem. 572 (2) (2004) 433–440, https://doi.org/10.1016/j.jelechem.2004.07.016.

[117] D.F. Roeper, D. Chidambaram, C.R. Clayton, G.P. Halada, Development of an environmentally friendly protective coating for the depleted uranium–0.75 wt% titanium alloy Part II: coating formation and evaluation, Electrochim. Acta 51 (3) (2005) 545–552, https://doi.org/10.1016/j.electacta.2005.05.015.

[118] D. Rodriguez, R. Mishra, D. Chidambaram, Molybdate-based conversion coatings for aluminum alloys Part I: coating formation, ECS Trans. 45 (28) (2013) 1–12, https://iopscience.iop.org/article/10.1149/04528.0001ecst/meta.

[119] D. Rodriguez, R. Mishra, D. Chidambaram, Molybdate-based conversion coatings for aluminum alloys Part II: coating chemistry, ECS Trans. 45 (19) (2013) 91–103, https://iopscience.iop.org/article/10.1149/04519.0091ecst/pdf.

[120] J.A. Wharton, D.H. Ross, G.M. Treacy, G.D. Wilcox, K.R. Baldwin, An EXAFS investigation of molybdate-based conversion coatings, J. Appl. Electrochem 33 (7) (2003) 553–561, https://doi.org/10.1023/A:1024911119051. https://link.springer.com/article/.

[121] C.-S. Liang, Z.-F. Lv, Y.-L. Zhu, S.-A. Xu, H. Wang, Protection of aluminium foil AA8021 by molybdate-based conversion coatings, Appl. Surf. Sci. 288 (1) (2014) 497–502, https://doi.org/10.1016/j.apsusc.2013.10.060.

[122] X. Chen, S. Xu, Growth process of molybdate conversion coating on the surface of aluminum foil and its adhesive mechanism, Surf. Interface Anal. 53 (8) (2021) 1048–1058, https://doi.org/10.1002/sia.7006.

[123] S. Yang, S. Li, Y. Meng, M. Yu, J. Liu, B. Li, Corrosion inhibition of aluminum current collector with molybdate conversion coating in commercial $LiPF_6$-esters electrolytes, Corros. Sci. 190 (9) (2021) 109632, https://doi.org/10.1016/j.corsci.2021.109632.

[124] S.J. Mao, W.F. Li, X.R. Zeng, A.H. Yi, Z.M. Liao, W. Zhu, Multiple transitional metal oxides conversion coating on AA6063 toward corrosion protection and electrical conductivity, Surf. Coat. Technol. 397 (9) (2020) 125189, https://doi.org/10.1016/j.surfcoat.2020.125819.

[125] A.S. Hamdy, A.M. Beccaria, P. Traverso, Corrosion protection of AA6061 T6-10% Al_2O_3 composite by molybdate conversion coatings, J. Appl. Electrochem 35 (5) (2005) 467–472. https://link.springer.com/article/10.1007/s10800-004-8329-3.

[126] Y. Huang, S. Mu, Q. Guan, J. Du, Corrosion resistance and formation analysis of a molybdate conversion coating prepared by alkaline treatment on aluminium alloy 6063, J. Electrochem. Soc. 166 (8) (2019). C224-C230, https://iopscience.iop.org/article/10.1149/2.1111908jes.

[127] T. Kosaba, I. Muto, M. Nishimoto, Y. Sugawara, Chemical conversion treatment of AA5083 aluminum alloy and AISI 1045 carbon steel under galvanically coupled condition in Na_2MoO_4: effect of pH on corrosion resistance, Mater. Trans. 64 (2) (2023) 568–577, https://doi.org/10.2320/matertrans.MT-M2022163.

[128] K. Sayin, D. Karakaş, Quantum chemical studies on the some iorganic corrosion inhibitors, Corros. Sci. 77 (12) (2013) 37–45, https://doi.org/10.1016/j.corsci.2013.07.023.

[129] F. Rahimi, M. Rezai, Electrochemical studies and molecular simulations on the use of molybdic acid for stabilization of AISI 304 stainless steel passive film in sulfuric acid medium, J. Mol. Liq. 344 (12) (2021) 117733, https://doi.org/10.1016/j.molliq.2021.117733.

[130 F. Rahimi, M. Rezai, Improving the localized corrosion resistance of 304 stainless steel in HCl solution by adsorption of molybdate ions: interaction mechanisms at the interface using molecular dynamics simulation and electrochemical noise analysis, Colloids Surf. A 647 (12) (2023) 129085, https://doi.org/10.1016/j.molliq.2021.117733.